

FIRE: A Failure-Adaptive Reinforcement Learning Framework for Edge Computing Migrations

Marie Siew, Shikhar Sharma, Zekai Li, Kun Guo, *Member, IEEE*, Chao Xu, *Member, IEEE*, Tania Lorido-Botran, Tony Q.S. Quek, *Fellow, IEEE*, Carlee Joe-Wong, *Senior Member, IEEE*



Abstract—In edge computing, users' service profiles are migrated due to user mobility. Reinforcement learning (RL) frameworks have been proposed to do so, often trained on simulated data. However, existing RL frameworks overlook occasional server failures, which although rare, impact latency-sensitive applications like autonomous driving and real-time obstacle detection. Nevertheless, these failures (rare events), being not adequately represented in historical training data, pose a challenge for data-driven RL algorithms. As it is impractical to adjust failure frequency in real-world applications for training, we introduce FIRE, a framework that adapts to rare events by training a RL policy in an edge computing digital twin environment. We propose ImRE, an importance sampling-based Q-learning algorithm, which samples rare events proportionally to their impact on the value function. FIRE considers delay, migration, failure, and backup placement costs across individual and shared service profiles. We prove ImRE's boundedness and convergence to optimality. Next, we introduce novel deep Q-learning (ImDQL) and actor critic (ImACRE) versions of our algorithm to enhance scalability. We extend our framework to accommodate users with varying risk tolerances. Through trace driven experiments, we show that FIRE reduces costs compared to vanilla RL and the greedy baseline in the event of failures.

Index Terms—Edge Computing, Service migration, Resilient Resource Allocation

1 INTRODUCTION

Mobile (or multi-access) edge computing (MEC) is a key technology in 5G and 6G telecommunication systems. It enables computationally intensive and latency sensitive mobile applications such as real time image processing, augmented reality, interactive gaming, etc. In MEC, computing resources such as server clusters are positioned close to end-users, typically at cellular base stations or WiFi access points

at the network edge of the radio access network [1], [2]. This proximity enables latency sensitive applications, by avoiding wide-area network delays encountered in cloud computing [2].

Researchers have been actively investigating how to jointly allocate computing and radio resources to computing tasks offloaded to edge servers [1], [3]–[6]. Nevertheless, user mobility across geographical areas presents a challenge towards task offloading [7]–[10]. Service migration, moving service profiles to access points nearer the user as they move, has been proposed to help reduce latency and maintain service continuity [8], [9]. Yet, frequent service migration in response to user movement causes additional expenditure, due to the increase in energy consumption. Therefore, balancing the delay-migration cost tradeoff in service migration has been widely studied [7], [8], [11]–[15]. Due to the large decision space of possible migrations when the numbers of access points and time-slots increase, and the lack of information on costs and mobility patterns, markov decision processes (MDPs) and reinforcement learning (RL) are used as common solution methods [7], [11], [16], [17]. Such methods often rely on digital twins of the edge computing network to train RL models, as digital twins allow the exploration of different resource allocation policies, without generating real-world consequences.

1.1 Challenges: Edge Computing and Resilience

RL-based solutions to resource management in edge computing rely on a realistic simulation of the edge computing environment. Few migration works, however, account for another challenge in edge computing: the resilience of edge computing systems to *rare but serious events like server failures*. They occur due to reasons such as system overload, hardware failures, or malicious attacks, and they can be costly: the average cost of an outage at a cloud data center, for example, has increased to \$740000 in 2016 [18]. Edge server failures may be even more probable than those in the cloud due to their distributed geographical locations, which complicates management and maintenance [19], though they will likely remain rare overall. Even worse, however, edge computing failures can have a sizeable impact as many

Marie Siew and Tony Q.S. Quek are with the Information Systems and Technology and Design Pillar, Singapore University of Technology and Design, Singapore 487372.

Shikhar Sharma, Zekai Li, and Carlee Joe-Wong are with the Electrical and Computer Engineering department, Carnegie Mellon University, 15213 Pittsburgh, PA, USA.

Kun Guo is with the Shanghai Key Laboratory of Multidimensional Information Processing, School of Communications and Electronics Engineering, East China Normal University, Shanghai 200241, China.

Chao Xu is with the School of Information Engineering, Northwest A&F University, Yangling 712100, China.

Tania Lorido-Botran is with Roblox, USA.

edge computing applications are latency sensitive, such as the Internet of vehicles, augmented reality, and video processing applications [1]. Managing resources without considering rare but severe failure increases latency and reduces reliability. For instance, if the user's service profile is migrated to an access point that then experiences a server failure, its job is not able to be completed, jeopardizing the smooth and safe functioning of applications, such as autonomous driving and real time obstacle detection.

Therefore, we need a technique to handle failures, to ensure uninterrupted application operation. We propose the use of *backups*, which can take over when the primary service's edge server fails. Nevertheless, managing the migration of both the primary and backup services is challenging, especially as the number of access points and timeslots increases. Additionally, the network operator has a lack of knowledge of the user mobility distributions and associated costs. As mentioned above, MDP and RL has traditionally been proposed as a method to solve the service migration problem [7], [11], [16], [17]. Nevertheless, rare events and failures occur at a low probability, making it difficult to jointly plan or learn an optimal resource allocation policy for both the usual and rare event scenarios. This is because *reinforcement learning's reliance on past reward data may overlook the significance of rare events, impacting the training process.* [20]. Therefore, we introduce **FIRE**: Failure-adaptive Importance sampling for Rare Events, a *resilience* framework for edge computing service migration.

1.2 FIRE: Failure-adaptive Importance sampling for Rare Events

Our FIRE framework employs a digital twin - inspired setup, employing reinforcement learning to optimize service migration and the *backup migration* in edge computing systems, amidst potential rare service failures. A digital twin edge computing system virtually replicates a physical edge computing system and mirrors its network conditions, akin to similar setups used for data center management and remote monitoring [21]. Our framework FIRE further models limited edge server capacity and communication delays to allow the exploration of service and backup migration optimization in the network, in light of rare event states. Our optimization balances the trade-offs amongst the following costs: *communication and computing delay costs* of the multiple users, the *migration cost* of service profiles, the *backup storage and migration costs*, along with the *failure costs*. Because the actual rare event probability is low and unable to help us learn an optimal policy to prepare for rare events, we use *importance sampling of rare events* in our digital twin setup to increase the sampling of the rare events in the reinforcement learning environment. We sample at a rate which represents their contribution to system wide costs, to help us prepare for rare events. Error correction is done through the use of importance sampling weights, to enable us to learn an optimal policy with respect to the true rare events probability. Unlike online training, training of RL in the edge computing digital twin also enables the system to learn policies while *avoiding the large failure costs* such as the high cost experienced by latency sensitive applications during server failures. The converged policy trained by the

simulator is then applied to online scenarios, in which rare events happen at their natural probabilities.

We model two decision making scenarios. Firstly, we suppose that every user has an individual service profile for job computation. Secondly, we consider multiple users sharing service profiles, for example common game environments when users are playing the same mobile or AR game together, or users sharing common neural networks for multi-modal learning [22]. The service profile replicas can also serve as backups in this second scenario [23], while in the first scenario we must create an individual backup for each user. We further consider that edge computing users may exhibit varying risk tolerances due to differences in their computing applications and latency requirements. Some users, for example, may have a higher risk tolerance for edge server failures due to their application being less latency sensitive than others, or may be less willing to incur a cost of placing and migrating backups to prepare for failures. In light of this, we propose an algorithm that caters to users of different risk tolerances, without requiring separate RL algorithm training for different risk tolerances.

In summary, the **contributions** of this paper are as follows:

- We present a **model** of service migration and backup placements given user mobility that introduces the modelling of server failures as rare events. We model the setting where all users have individual service profiles, and the setting where users share service profiles.
- We introduce **FIRE**, a *resilience* framework designed to handle rare events like server failures. As a digital twin, our importance sampling based Q-learning algorithm **ImRE** simulates rare events frequently without real-world consequences, allowing us to learn a failure-aware migration policy with reinforcement learning. We prove that this algorithm is bounded (Theorem 2), and that it converges to the optimal policy (Theorem 4).
- We propose deep Q-learning (**ImDQL**) and actor critic (**ImACRE**) versions of our importance sampling-based rare events adaptive algorithm, to handle large and combinatorial state and action spaces in real-world networks. These algorithms differ from traditional deep Q-Learning and actor critic as we incorporate importance sampling and error correcting weights. Additionally, we present the **RiTA** algorithm that adjusts service migration and backup placement based on individual risk tolerance.
- Finally, we provide **trace-driven simulation results** showing the convergence of our algorithms to optimality. We show that unlike vanilla Q-learning, our algorithm is able to be resilient towards server failures, resulting in sizeable cost reductions. Our importance sampling framework is able to be extended and modified, to tackle other resource allocation and decision making problems in light of rare events in networking and communications.

The paper is structured as follows. Section 2 discusses the related work. Section 3 and 3.2.2 present the system models. Section 5 presents the problem formulation. Follow-

ing which, we present our solution and its proofs in Section 6, and the deep Q-learning and Actor Critic algorithms in Section 7. Next, Section 8 addresses the heterogeneous risk tolerance scenario. Finally, we present simulation results in Section 9 and conclude in Section 10.

2 BACKGROUND AND RELATED WORK

Building on the literature on service and virtual machine (VM) migration in follow-me-cloud [24], [25], **service or VM placement and migration** in light of user mobility in edge computing has been a widely studied problem [7]–[9], [11]–[16]. These are often NP-hard knapsack-like problems. In particular, [7], [11] put forth an MDP formulation to make optimal migration decisions in light of unknown mobility information, with [11] using dynamic programming and reinforcement learning to find the optimal solution. [8] optimized the performance-cost tradeoff in service migration in the long run via Lyapunov optimization. [13] formulated a personalized performance service migration problem as a multi-armed bandit problem. Nevertheless, these service migration works have not approached the problem from the angle of resilience, preparing for and being adaptive to server failures.

At the same time, other works have realized that **cloud and edge computing presents resilience challenges**, particularly regarding resource allocation [26]. Ultra-reliable offloading mechanisms have been proposed to address this challenge using two-tier optimization [27]. Proactive failure mitigation has also been proposed for edge-based NFV [28]. Failure aware workflow scheduling has been proposed for cloud computing [29]. Others have examined the use of reinforcement learning for replica placement in edge computing [30] and caching placement [31]. The migration of users at overlapping coverage areas to other servers has been considered in [32], but under this scheme, the users in the center of coverage areas still experience a higher latency as they are connected to the cloud. [18] used graphical models to learn spatio-temporal dependencies between edge server and link failures. Nevertheless, the above works did not consider resource allocation in light of unknown user mobility across different locations, or the cost of service migration. Our prior work [33] considers rare events in service migration, for a single user scenario, introducing an actor critic importance sampling algorithm. In this work, we extend the framework to consider more intricate multiple user scenarios, including individuals with both individual and shared service profiles. We also introduce tabular and deep Q-learning importance sampling algorithms, and provide theoretical guarantees for the tabular algorithm.

Other problems in edge computing have been investigated from the **risk-awareness** perspective as well, catering to heterogeneous users and applications, for example risk-aware non-cooperative MEC offloading [34], risk-aware energy scheduling in edge computing [35], and energy budget risk-aware application placement [36]. However, they do not consider the effect of rare events on learned RL policies.

(Deep) reinforcement learning has been used to optimize migration and offloading in edge computing [7], [11], [16], [17], [37], [38], with the goal of minimizing migration costs and satisfying edge resource constraints while

maximizing quality-of-computation [37] or trading off the expended energy and latency [38]. Importance sampling is widely used in reinforcement learning for policy evaluation (i.e., finding the expected future reward from following a given policy π) [39], and prior work has proposed to utilize importance sampling to over-sample rare events for policy evaluation [20]. However, these two works involve estimating the value function given a fixed policy, and does not consider learning the optimal policy π^* which entails policy changes. Their proof techniques do not generalize to the Q-learning [40] that forms the core of FIRE. Recent work has proposed using importance sampling to enhance RL's data efficiency [41] in more general settings, but they do not consider rare events explicitly and use a technique that requires knowledge of the full system dynamics.

3 SERVICE MIGRATION OF INDIVIDUAL SERVICE PROFILES IN LIGHT OF RARE EVENTS

In this section, we introduce our failure-aware service migration model, where users have their individual service profiles. In the next section, we will consider users that share service profiles.

3.1 Service Placement Model

Users and edge servers. We consider an MEC system with K users and N access points (APs), such as a base station or wifi-access point. Each access point is equipped with a server to which users can offload their time-sensitive computing jobs, and we associate each access point with a disjoint physical region; users in this region then connect to this access point. Users are mobile and move from region to region at different times of the day. For example, office workers may move to the city districts for work during morning rush hours. This influences which access point they will be nearest to. User k 's location at time t is represented by $l_u^k(t)$. We consider that each user will be associated with its nearest access point, via local area network (LAN). The users' mobility pattern follows a probability distribution $m(l_u^k | l_u^k)$, where $m(l_u^k | l_u^k)$ represents the transition probability the user travels to location l_u^k , after being at location l_u^k .

Each user maintains a *service profile* at the edge servers, e.g., in virtual machines or containers [8], [42], that consists of the state needed to run its edge computing application. Our goal is then to decide where the service profile and any backups should be located. To maintain low latencies for time-sensitive service applications, in light of user mobility, services are pre-migrated - likely to nearby APs. Service migration is stateful, involving the migration of the set of parameters associated with the user, along with the computing job's intermediate results. At each time-slot t , the user sends a service request to the network operator. The location of the user's service at time t is represented by $l_s^k(t)$, and due to pre-migrations the network operator makes this placement decision in advance, before knowledge of the user location at time t is known.

Failure model. In reality, rare events (system anomalies) such as server failures or shutdowns occur. Such events will impact the quality of service the user receives, as the user

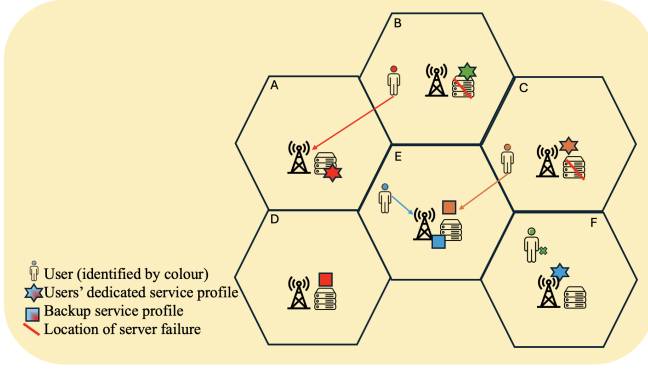


Fig. 1. Each user has its individual service profile, which has a backup, in case the server where there service profile is at fails.

is not able to have his or her job computed on time, or at all, impacting the safe and smooth functioning of edge applications and jeopardizing the low latency benefits of edge computing.

We consider two server types in the network. The first type models larger edge datacenters, which tend to have more safety mechanisms like fully duplicated electrical lines with transfer switches that help servers come back online fast after a failure, causing just a slight delay to users. The second type models a smaller edge data center that is less equipped with mechanisms to help deal with failure. These servers take longer to come back online, resulting in a longer delay and higher probability of jobs not being served at all, hence a higher cost. We let $f_{ind}^k(t)$ represent the failure indicator, which indicates whether $l_s^k(t)$, the location of user k 's service profile, experiences failure at time t . Failures are Markovian, and under Server Type two, there is a higher probability of failures continuing into the next time-slot.

To take into account the potential failures and reduce the costs experienced by the user, a **backup** of the user's service profile can be placed in the system. This way, if the server $l_s^k(t)$ at which user k 's service is placed at experiences a failure, the user will still be able to offload its job. As seen in Fig. 1, unlike the green user which does not have a backup service profile, the brown user is still able to offload its job computation even though the server at AP C failed, because there is a backup at location E.

We formulate a **Markov Decision Process (MDP)** in which the system state $s(t) \in S$ is $[s_1(t), \dots, s_K(t), \dots, s_K(t)]$, where

$$s_k(t) = (l_u^k(t), l_s^k(t), f_{ind}^k(t), b_{ind}^k(t)). \quad (1)$$

l_u^k is user k 's current location, l_s^k is the location of user k 's service, f_{ind}^k is an indicator on whether the user's service is placed at a location with a server failure, and b_{ind}^k indicates whether there currently is a backup for user k 's service in the system. At each timeslot t , the network operator takes action $a(t) = [a_1(t), \dots, a_K(t), \dots, a_K(t)]$, where

$$a_k(t) = (l_s^k(t+1), b_u^k(t+1)) \quad (2)$$

pre-emptively, before the users moves to their next locations $[l_u^k(t+1)]$. This involves determining the placement location of the service $l_s^k(t+1)$, and the position of the backup in the system $b_u^k(t+1) \in \{0, 1, \dots, N, \text{no backup}\}$. These decisions will directly impact the system state s at the next timeslot.

Transitions between states are governed by users' movements from one access point ($l_u^k(t)$) to another ($l_u^k(t+1)$) following their mobility distribution $m(l_u^k|l_u)$. To quantify these transitions, we let

$$h(\tilde{s}|s, a) = Pr(a) \prod_{k=1}^K m(l_u^k|l_u), \quad (3)$$

the product of the user's mobility distribution and the probability that the network operator takes a particular action, where $\tilde{s}(t) = [\tilde{s}_1(t), \dots, \tilde{s}_K(t), \dots, \tilde{s}_K(t)]$ and

$$\tilde{s}_k(t+1) = (l_u^k(t+1), l_s^k(t+1), b_{ind}^k(t+1)) \in \tilde{S} \quad (4)$$

refers to the state record without the failure indicator f_{ind} . We let the set of these 'state records' be \tilde{S} . At each state s , there is a small probability of $\epsilon(s)$ (for example $\epsilon(s) = 0.01$), that in the next timeslot, a server failure occurs at at least one location. The failure indicator f_{ind} is 1 when the location of at least one service profile $l_s^k(t)$ experiences a server failure. These states belong to the set of "Rare event states", $T \subset S$, defined as follows:

Definition 1. A subset of states $T \subset S$ is called the Rare Event State Set if the following properties hold:

1. There exists $s \in S, s' \in T$ for which $p(s'|s, a) > 0$.
2. Let $T^\pi(s)$ denote the contribution of the rare states towards the value of state s , according to Eq. (22). For a given policy π , there exists $s \in S$ for which

$$|T^\pi(s)| \gg 0 \quad (5)$$

3. For every $s' \in T$, $f_{ind} = 1$, indicating that the location of at least one user's service profile l_s^k is experiencing a failure.

Property 1 means that transition to the rare event state set T is possible. Property 2 means that the rare event states (set T) collectively have a sizeable (non-negligible) impact on the value function and hence on the system's cost.

With a larger probability of $1 - \epsilon(s)$, no server failure occurs, i.e. $f_{ind} = 0$. The non rare event states "Normal States" are defined as the set $S \setminus T$. Hence we have

$$\begin{aligned} s_k(t+1) &= \tilde{s}_k(t+1) \cup f_{ind}^k(t+1) \\ &= (l_u^k(t+1), l_s^k(t+1), b_{ind}^k(t+1), f_{ind}^k(t+1)) \end{aligned} \quad (6)$$

Therefore, the overall state transition probability of the system can be expressed as

$$p(s'|s, a) = \begin{cases} (1 - \epsilon(s))h(\tilde{s}|s, a), & \text{if } s' \notin T \\ \epsilon(s)h(\tilde{s}|s, a), & \text{if } s' \in T, \end{cases} \quad (7)$$

3.2 Reward Function

We next specify the reward function of our MDP. We aim to learn a policy that minimizes the total cost of the migration policy, including both operational costs and failure and backup costs.

3.2.1 Operational Costs

The network operator migrates the users' profiles across access points, to deliver a better QoS (lower job delay) for the user. We first model the costs incurred in normal (non-failure) states, which include communication and computing delays, both of which affect user QoS, as well as the

cost of migrating service profiles. We let $d_{l_u, j}^{\text{comm}, k}$ denote the communication delay the user faces when it offloads its job to the edge server, given that its current location is l_u^k and its service is placed at access point j . $d_{l_u, j}^{\text{comm}, k}$ consists of the access latency of uploading the job to the user's associated access point, and the transfer latency of forwarding the job to the edge server's location if the service is placed at another access point (i.e. $l_u^k \neq j$). This transferring latency via LAN depends on the hop count of the shortest communication path [13]. Therefore, the delay is a function of the distance between l_u^k and j . Therefore, the **total communication delay cost of K users** at time t is

$$D(t) = \sum_{k=1}^K \sum_j d_{l_u^k, j}^{\text{comm}} \mathbb{1}_{\{l_s^k(t)=j\}}, \quad (8)$$

where $\mathbb{1}_{\{l_s^k(t)=j\}}$ is the indicator function, which will take the value of 1 if the user's service profile is placed at access point j , and will take the value of 0 otherwise.

As multiple users share the resources at an edge node, users will experience a compute delay cost. Modelling the process at each AP as an M/M/1 queue [43], the **total computing delay experienced across all APs** at time t is [12]:

$$C(t) = \sum_{j \in A} \sum_{k=1}^K \mathbb{1}_{\{l_s^k(t)=j\}} \frac{1}{x_j - \sum_{k=1}^K z_k \mathbb{1}_{\{l_s^k(t)=j\}}} \quad (9)$$

where x_j refers to the capacity at AP j , z_k is user k 's task size, and $\sum_{k=1}^K z_k(t) \mathbb{1}_{\{l_s^k(t)=j\}}$ is the total load at AP j at time t . The total computing delay is the sum over all locations j and users k , of the average queuing delay each user experiences. As users share computing resources at an AP, the presence of other users' jobs will impact the queuing (i.e. computing) delay experienced by a user.

Service profiles are not migrated greedily along with the user, because doing so incurs a service migration cost for the network operator, requiring the operator to balance the communication delay and migration cost. The migration cost $m_{i,j}$, which includes the operational and energy costs on network devices like routers and switches [8], is a function of the distance across two access points i and j . Hence, the **total migration cost of K users** at time t is

$$M(t) = \sum_{k=1}^K \sum_{i \in A} \sum_{j \in A} m_{i,j} \mathbb{1}_{\{l_s^k(t-1)=i\}} \mathbb{1}_{\{l_s^k(t)=j\}}, \quad (10)$$

where $\mathbb{1}_{\{l_s^k(t-1)=i\}}$ is the indicator function which will take the value of 1 if the service profile was placed at location (access point) i at time $t-1$.

3.2.2 Failure and Backup Costs

We next specify the costs incurred by provisioning backups in case of failures.

Backup costs. There is a cost $B(t)$ incurred by storing the backup at a server. This cost is a sum of the backup

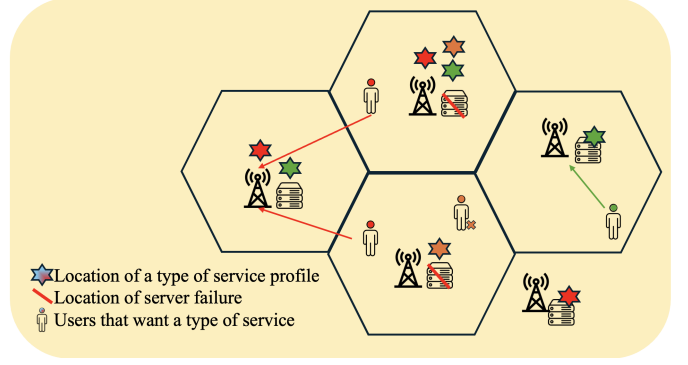


Fig. 2. Multiple users share a service profile for their task application, e.g. a common game environment or neural network. For instance, the users in red share the service profile in red, which has multiple copies in the network.

migration cost and the backup storage cost, as it takes up space and prevents other content from being stored.

$$B(t) = \sum_{k=1}^K \sum_{j \in A} \rho_j \mathbb{1}_{\{b_u^k(t)=j\}} + \sum_{k=1}^K \sum_{i \in A} \sum_{j \in A} m_{i,j} \mathbb{1}_{\{b_u^k(t-1)=i\}} \mathbb{1}_{\{b_u^k(t)=j\}}, \quad (11)$$

where ρ_j is the storage cost at access point j . There is also a **failure cost $F(t)$** incurred

$$F(t) = \sum_{k=1}^K F \mathbb{1}_{\{f_{ind}^k(t)=1\}} (\mathbb{1}_{\{b_u^k(t)=\text{no backup}\}} \vee \mathbb{1}_{\{b_u^k(t)=l_s^k(t)\}}) \quad (12)$$

The **failure cost F** is experienced at time t when 1) location $l_s^k(t)$ has a failure at time t ($f_{ind}^k(t) = 1$), and b) there is no backup in the system ($b_u^k(t) = \text{no backup}$), or when the placement of the backup $b_u^k(t)$ equals the location of the main service $l_s^k(t)$. Otherwise, if there is a backup placed, there will be no failure cost experience, and the cost will be much lower. Note, however, that the presence of failures themselves, i.e., $f_{ind}(t)$, is independent of the user actions.

4 SERVICE MIGRATION OF SHARED SERVICE PROFILES IN LIGHT OF RARE EVENTS

In certain scenarios, multiple users share a common service profile (SP) for the same task. This could take the form of a common neural network for multi-modal learning, or a common game environment for their Augmented Reality (AR) or mobile gaming applications such as when multiple users are playing a game together [22]. Therefore, the network operator is concerned with the placement of shared SPs across the network, in light of the geographical demand distributions of the different SPs. In the event of a server failure, the impact will be multiplied when SPs are shared, as more users cannot have their job served.

As in the case of individual service profiles, we formulate a **Markov Decision Process (MDP)** in which the system state is $[s_{1,1}(t), \dots, s_{i,j}(t), \dots, s_{I,J}(t)]$, where for each location, SP pair (i, j) , their component of the state space at time t is

$$s_{i,j}(t) = (u_{i,j}(t), d_{i,j}(t-1), f_i(t), t_i(t)), \quad (13)$$

where $u_{i,j}(t)$ is the number of users who want to use SP j at location i , $d_{i,j}(t-1)$ indicates whether SP j has been previously deployed at location i , and $f_i(t)$ and $t_i(t)$ denote the failure status and the server type at location i respectively. Here, there are multiple identical copies of profiles being placed, as many users share them (see Fig. 2). Note that this state space (concatenation over all location - SP pairs) is different from that in the individual service profile scenario in Section 3 (concatenation over individual user information). Here the placement decisions depend on the location and mobility distributions of the users who *share* the profile, whereas in Section 3 the placement of every profile is dependent on the location of the corresponding individual user. The corresponding action space will be

$$[(l_{loc1}^{SP1}, l_{loc2}^{SP1}, \dots, l_{locN}^{SP1}), \dots, (l_{loc1}^{SPj}, l_{loc2}^{SPj}, \dots), \dots], \quad (14)$$

where $l_{loc i}^{SPj} \in \{0, 1\}$ is a binary variable indicating whether we place or migrate SP j at location i .

As in the case of individual service profiles, we aim to learn a policy that minimizes the total costs, which include both operational and backup and failure-related costs.

The **total communication delay** cost across all SP types $j \in SP$ and locations $i \in A$, at time t is

$$D^{sh}(t) = \sum_{j \in SP} \sum_{i \in A} u_{ij}(t) \min_{\hat{i} \in \{\hat{i} | l_{loc \hat{i}}^{SPj} = 1\}} d_{i, \hat{i}}^{comm}, \quad (15)$$

where $d_{i, \hat{i}}^{comm}$ is the communication delay from location i to \hat{i} , same as Section 3. The users at location i access the nearest AP which contains the SP type they require ($\min_{\hat{i} \in \{\hat{i} | l_{loc \hat{i}}^{SPj} = 1\}} d_{i, \hat{i}}^{comm}$). User QoS is also affected by the **total computing delay experienced across all APs** at time t , which is [12]:

$$C^{sh}(t) = \sum_{i \in A} \frac{1}{x_i - \sum_{j \in SP} \sum_{\hat{i} \in A} load_{j, \hat{i}}(t)} \quad (16)$$

where x_i is the capacity of the servers at AP i . The load at each location i is a sum over all SP types j , all other locations \hat{i} (inclusive of i). The load $load_{j, \hat{i}}(t) = z_j u_{i, j}(t) \wedge \mathbb{1}_{\{\hat{i} = \text{argmin}_{\{m | l_{loc m}^{SPj} = 1\}} d_{m, \hat{i}}^{comm}\}}$, the product of task j 's size z_j , the number of users at location \hat{i} who need SP type j , $u_{i, j}(t)$, and the indicator function indicating that location \hat{i} is the nearest location containing SP j , to the users at \hat{i} . As in the case of individual service profiles, service profiles at the same AP must share resources, leading to increased delays.

The **total migration cost** at time t of required migration is

$$M^{sh}(t) = \sum_{j \in SP} \mathbb{1}_{\{d_{i, j}(t-1)=0 \ \& \ d_{i, j}(t)=1\}} \times [g_{cloud, i} \mathbb{1}_{\{d_{i, j}(t-1)=0, \forall \hat{i}\}} + \min_{\{\hat{i} | d_{i, j}(t-1)=1\}} m_{\hat{i}, i} \mathbb{1}_{\{\exists \hat{i} \text{ s.t. } d_{i, j}(t)=1\}}].$$

The migration cost for SP j kicks in if it is to be placed at location i at time t and was not placed there at $t-1$ (i.e. $d_{i, j}(t-1) = 0$ & $d_{i, j}(t) = 1$). It consists of either downloading SP j from the cloud server for a new deployment when $d_{i, j}(t-1) = 0, \forall \hat{i}$, or migrating SP j from the nearest location \hat{i} when $\exists \hat{i} \text{ s.t. } d_{i, j}(t) = 1$. The **total storage cost** of storing all the deployed SPs is

$$S^{sh}(t) = \sum_{j \in SP} \sum_{i \in A} h_j \rho_i \mathbb{1}_{\{l_{loc i}^{SPj}(t)=1\}}, \quad (17)$$

where h_j is the size of service profile type i and ρ_i is the per unit storage cost at AP i . The **failure cost** is incurred for the users who need to use service profile type j when either a) SP type j is not placed anywhere ($l_{loc i}^{SPj} = 0 \ \forall i$), b) the delay exceeds del^j , the delay threshold for this application ($\min_{i \in \{\hat{i} | l_{loc \hat{i}}^{SPj} = 1\}} d_{i, \hat{i}}^{comm} > del^j$), or c) there is a failure at a location \hat{i} , and there is no available SP j placed elsewhere, or the minimum delay elsewhere exceeds the delay threshold del^j for this application.

$$F^{sh}(t) = \sum_{j \in SP, i \in A} u_{ij} [\mathbb{1}_{\{l_{loc i}^{SPj} = 0 \ \forall i\}} \vee \mathbb{1}_{\{\min_{i \in \{\hat{i} | l_{loc \hat{i}}^{SPj} = 1\}} d_{i, \hat{i}}^{comm} > del^j\}} \vee \Pi_{\hat{i}}(\mathbb{1}_{\{f_i(t)=1\}}) \wedge (\mathbb{1}_{\{l_{loc i}^{SPj} = 0 \ \forall \hat{i} \neq i\}} \vee \mathbb{1}_{\{\min_{i \in \{\hat{i} \neq i | l_{loc \hat{i}}^{SPj} = 1\}} d_{i, \hat{i}}^{comm} > del^j\}}))]$$

5 COST MINIMIZATION IN LIGHT OF RARE EVENTS

In this section, we introduce the service migration optimization problems, for both the individually used (Section 3) and shared (Section 3.2.2) service profile scenarios. Our focus is on long term service placements and backup storage decisions, taking into account potential rare events such as server shutdowns which have an impact on the user experience. For both problems, we aim to minimize the expected sum of the **weighted sum of the communication and computing delay, migration, storage and failure costs**. Actions are taken in a digital twin framework, as they allow for algorithm training while avoiding the cost of failures in real-world applications. Firstly, we introduce the optimization problem for the scenario where all users have their individual service profiles.

$$\min_{\pi(s)} \mathbb{E}_{\pi} \left[\sum_t (w_D D(t) + w_C C(t) + w_M M(t) + w_B B(t) + w_F F(t)) \right] \quad (18)$$

$$\text{s.t. } [s_1(t), \dots, s_k(t), \dots, s_K(t)] \sim p(s'|s, a). \quad (19)$$

Eqs.(8), (10), (9), (11), (12),

where w_D, w_C , etc. are the corresponding weights, which can be adjusted based on the priority of different costs. The decision variable $\pi(s, a) = \{P_r(a_t = a | s_t = s)\}$ is the network operator's policy, the probability it will take each action $a(t)$ (service placement and backup storage decision for all users) given the state $s(t)$. The first constraint indicates that the state dynamics follows the transition probability of the system in Eq. (7), incorporating rare event transitions, while the other constraints indicate the delay, migration, backup and failure costs respectively. Next, we introduce the optimization problem for the scenario where users share service profiles; note that we aim to minimize the same types of costs as in Eq. (18) with individual service profiles.

$$\min_{\pi(s)} \mathbb{E}_{\pi} \left[\sum_t (w_D D^{sh}(t) + w_C C^{sh}(t) + w_M M^{sh}(t) + w_S S^{sh}(t) + F^{sh}(t)) \right] \quad (20)$$

$$\text{s.t. } [s_{1,1}(t), \dots, s_{i,j}(t), \dots, s_{I,J}(t)] \sim p(s'|s, a). \quad (21)$$

Eqs.(15), (17), (16), (17), (18).

The decision variable $\pi(s, a)$ is the network operator's policy, the probability it will take each action $a(t)$ (placement decisions of the service profiles) given the current state $s(t)$. The first constraint indicates that the state dynamics follows the system's transition probability, which incorporates rare event transitions, while the other constraints indicate the delay, migration, storage and failure costs.

Proposition 1. *The number of migration path possibilities grows at least fast as $O(N^T)$.*

Proof. For each timeslot t , there are N possible locations to migrate a service profile. Since the service profile must be placed at a server each timeslot, the result follows. \square

Deciding a migration path for the user across T timeslots is similar to the shortest path problem. However, the network operator may not have information on mobility distributions and the corresponding latency costs, complicating look-ahead solutions. Since the costs of different users are coupled through service profiles' sharing of AP resources and consequent computing delays (see Eqs. (9) and (16)), finding the optimal migration strategies becomes yet more difficult. Thus, Markov Decision Processes and Reinforcement Learning have been used to derive service migration policies in the edge computing literature [11], [16], [17]. The difficulty in our problem further arises as we model occasional server failures, which impact the smooth and safe functioning of applications. As these failures occur at a low probability, and because reinforcement learning relies on past reward data, the learner may miss the importance of these rare events and be unable to learn an optimal policy adaptive to server failures. We introduce our solution in the next section.

6 REINFORCEMENT LEARNING IN THE PRESENCE OF SERVER FAILURES

In this section, we present FIRE: Failure-adaptive Importance sampling for Rare Events, a reinforcement learning based framework in an edge computing digital twin, to optimize service migration and backup placement in light of potential server failures. We define rare events formally in Subsection 6.1, introduce importance sampling in Subsection ??, present our algorithm (ImRE) and its proof in Subsections 6.2 and 6.3 respectively, and present an eligibility traces version of the algorithm (ETAA) for faster convergence in the Appendix. We propose a Deep Q learning and Actor Critic version of our algorithm in Section 7 to accommodate large state and action spaces, e.g., for many servers or users across a long amount of time.

6.1 Rare Events And Their Impact On The Value Function

We are concerned with rare event states if they have a sizeable impact on the user experienced costs, i.e. if these states collectively have an impact on the value function. The value function $V^\pi(s) : S \rightarrow \mathbb{R}$ for the policy π is the expected-return of state s , i.e. it indicates how "good" (cost wise) a state is (based on the discounted sum of future rewards),

when π is used. The discount factor γ indicates how much the network operator cares about future vs current rewards.

$$V^\pi(s) = \mathbb{E}_{a_t, p(s'|s, a)} \left[\sum_{t=1}^{\infty} \gamma^k r(s(t), a(t), a(t+1)) | s_0 = s \right]$$

where the reward (cost) is the per-timeslot cost in (18) or (20). The value function is the solution to the recursive Bellman equation [40]:

$$V^\pi(s) = \sum_{a \in A} \pi(s, a) \sum_{s' \in S} p(s'|s, a) [r(s, a, s') + \gamma V^\pi(s')].$$

Defining $T^\pi(s)$ as the collective contribution of the rare states towards $V^\pi(s)$ [20] given a fixed policy π , where the rare states T are as defined in Section 3.1, we have

$$T^\pi(s) = \epsilon(s) \sum_{a \in A} \sum_{s' \in \tilde{S}} h(\tilde{s}'|s, a) \pi(a|s) [r(s, a, s') + \gamma V^\pi(s')] \quad (22)$$

Likewise, defining $U^\pi(s)$ as the collective contribution of the non-rare states (states in $S \setminus T$) towards the value of state s , given a fixed policy π , we have :

$$U^\pi(s) = (1 - \epsilon(s)) \times \sum_{a \in A} \sum_{s' \in \tilde{S}} \pi(a|s) h(\tilde{s}'|s, a) [r(s, a, s') + \gamma V^\pi(s')]. \quad (23)$$

The Q-value (action-value) of a state action pair (s, a) is the expected-return of taking action a at state s , following π .

$$Q^\pi(s, a) = \mathbb{E}_\pi \left[\sum_{k=1}^{\infty} \gamma^k r(s(t), a(t), s(t+1)) | s_t = s, a_t = a \right]. \quad (24)$$

$$Q^\pi(s, a) = \sum_{s' \in S} p(s'|s, a) [r(s, a, s') + \gamma \sum_{a' \in A} \pi(a'|s') Q^\pi(s', a')] \quad (25)$$

The optimal policy will achieve the minimum cost and minimum value function:

$$Q^*(s, a) = \min_{\pi} Q^\pi(s, a). \quad (26)$$

6.2 ImRE: Q-Learning in Light of Rare Events

In this subsection, we present our importance sampling based failure-adaptive algorithm. We use a digital twin-based simulator in order to avoid the large failure costs experienced during server failures in online scenarios, and the converged policy trained in the digital twin is then applied to online scenarios, in which rare events happen at their natural probabilities. Our algorithm performs importance sampling while increasing the rare event probabilities from $\epsilon(s)$ to $\hat{\epsilon}(s)$. The transition probabilities $h(\tilde{s}|s, a)$, which mostly depend on the user mobility probabilities (Eq. (3)), are obtained from historical data. We use importance sampling because if rare events such as server failures are sampled at their natural probabilities, the reinforcement learning algorithm is not able to converge to the optimal policy; in particular, it may decide that the storage cost isn't worth having backups. This can be catastrophic in the event of failures. In our numerical simulations in Section 9, we show that unlike our algorithm, a traditional RL algorithm is unable to train an optimal policy which avoids experiencing high cost in the event of failures (Figs. 4 - 6).

Idea behind algorithm: Firstly, we introduce importance sampling: when we want to calculate the expectation of a function $f(x)$, and the true distribution p is difficult to sample from, importance sampling involves sampling from another distribution q , to help compute $E[f(x)]$ [44]. Here, the expectation of $f(x)$ can be estimated as

$$E[f(x)] = \int f(x)p(x)dx \quad (27)$$

$$= \int f(x) \frac{p(x)}{q(x)} q(x)dx \quad (28)$$

$$\approx \frac{1}{n} \sum_i f(x_i) \frac{p(x_i)}{q(x_i)}. \quad (29)$$

When q is well crafted, variance in the estimates will be reduced. The use of importance sampling in temporal difference (TD) based RL was proposed in [20], [39], where the state transition probabilities followed distribution $q(s'|s, a)$ rather than the true distribution $p(s'|s, a)$. For our service migration and backup placement problem, we will sample the rare events at probability $\hat{\epsilon}(s)$ (analogous to $q(s'|s, a)$), a higher rate than $\epsilon(s)$ (analogous to $p(s'|s, a)$), which is the probability of visiting a rare event state from state s . This allows us to sample rare events at a rate proportional to their contribution to the value of state s . Unlike [20], [39]'s importance sampling based value estimation given a fixed policy, our aim is to iterate over policies and learn an optimal policy π^* through importance sampling based Q-learning.

Therefore, to obtain $\hat{\epsilon}(s)$, we define $T(s, a)$ as the contribution of the rare states $s' \in T$ towards the Q-value of the state action pair (s, a) , and $U(s, a)$ as the contribution of the normal states $s' \in S \setminus T$ towards the Q-value of the state action pair (s, a) :

$$T(s, a) = \epsilon(s) \sum_{\tilde{s}' \in \tilde{S}} h(\tilde{s}'|s, a) [r(s, a, s') + \gamma \max_b Q(s', b)] \quad (30)$$

$$U(s, a) = (1 - \epsilon(s)) \sum_{\tilde{s}' \in \tilde{S}} h(\tilde{s}'|s, a) [r(s, a, s') + \gamma \max_b Q(s', b)] \quad (31)$$

where $s' = \tilde{s}' \cup f_{ind}$. With this, we have the relationship $T(s, a) + U(s, a) = Q(s, a)$. A potential update equation would be $T(s, a) \leftarrow (1 - \alpha_T)T(s, a) + \alpha_T \epsilon(s)(r(s, a, s') + \gamma \max_b Q(s', b))$, where α_T is the learning rate.

Nevertheless, updating at the state action (s, a) level may lead to slower convergence, especially with an increasing number of access points, leading to an exponential increase in the state-action combinations. For example, with 9 access points, there will be 360 states and 90 actions, leading to 32400 state-action combinations. We can reduce this complexity by exploiting our earlier observation that *the probability of rare events (i.e., server failures) happening is independent of the actions chosen*. Therefore, we propose updating T and U (the contributions of the rare events and non-rare events respectively towards the Q-value) at the state level:

$$T(s) = \epsilon(s) \sum_{a \in A} \sum_{\tilde{s}' \in \tilde{S}} \pi(a|s) h(\tilde{s}'|s, a) [r(s, a, s') + \gamma \max_b Q(s', b)]$$

$$U(s) = (1 - \epsilon(s)) \times \sum_{a \in A} \sum_{\tilde{s}' \in \tilde{S}} \pi(a|s) h(\tilde{s}'|s, a) [r(s, a, s') + \gamma \max_b Q(s', b)]$$

These equations contain a sum over the actions. The relationship $U(s) + T(s) = \sum_a Q(s, a) \pi(a|s)$ holds. To help us obtain the importance sampling rare event rate $\hat{\epsilon}(s)$, We will use the following respective update equations for $T(s)$ and $U(s)$ in our algorithm:

$$T(s) \leftarrow (1 - \alpha_T)T(s) + \alpha_T \epsilon(s)(r(s, a, s') + \gamma \max_b \hat{Q}(s', b))$$

$$U(s) \leftarrow (1 - \alpha_U)U(s) + \alpha_U (1 - \epsilon(s))(r(s, a, s') + \gamma \max_b \hat{Q}(s', b)).$$

Importance sampling and correction: Based on the above, we will calculate the rare event importance sampling rate $\hat{\epsilon}(s)$ as follows:

$$\hat{\epsilon}(s) \leftarrow \min(\max(\delta, \frac{|T(s)|}{|T(s)| + |U(s)|}), 1 - \delta). \quad (32)$$

The bounds $(\delta, 1 - \delta)$ ensure sufficient rare event sampling. As importance sampling of rare events takes place according to $\hat{\epsilon}(s)$, $\hat{p}(s'|s, a)$ is the transition probability in our algorithm which incorporates importance sampling. It follows Eq. (4), with $\epsilon(s)$ being replaced by $\hat{\epsilon}(s)$.

Because the rare events are sampled at the probability $\hat{\epsilon}$ instead of their actual probability ϵ , we need a method of correction, in order to learn the optimal policy for the original system with transition probability $p(s'|s, a)$ (Eq. (7)). Importance sampling correction weights $w(s, a, s')$ will be used, when obtaining the temporal-difference (TD) error in Q-learning. They are obtained through:

$$w(s, a, s') \leftarrow \begin{cases} \epsilon(s)/\hat{\epsilon}(s), & \text{if } s' \in T, \\ (1 - \epsilon(s))/(1 - \hat{\epsilon}(s)), & \text{if } s' \notin T, \end{cases} \quad (33)$$

where $1 - \epsilon(s)$ is the probability that s' is a non-rare event state. The TD error will be

$$w_t(r(s, a, s') + \gamma \max_b \hat{Q}(s', b)) - \hat{Q}(s, a), \quad (34)$$

instead of the traditional Q-learning TD error $r(s, a, s') + \gamma \max_b \hat{Q}(s', b) - \hat{Q}(s, a)$.

Algorithm description: The algorithm is presented in Algorithm 1 (**ImRE**). Firstly, we initialise $\hat{Q}(s, a)$, $\hat{T}(s)$ and $\hat{U}(s)$ to be 0 (for all states), and $\hat{\epsilon}(s)$ to be $\frac{1}{2}$ for all states. We also initialise the learning rates $\alpha^t, \alpha_T^t, \alpha_U^t$. For every timeslot, the importance sampling rare event probability $\hat{\epsilon}(s)$ will determine whether or not a rare-event (failure) occurs. Thereafter, the rest of the state transition will occur according to the probability distribution $h(\tilde{s}|s, a)$, where $\tilde{s}(t) = (l_u(t), l_s(t), b_{ind}(t))$. This would result in a new state s^{t+1} , and a reward value $r^{t+1} = r(s^t, a^t, s^{t+1})$ (line 4). Based on the next state s^{t+1} , a new action is selected according to the β -greedy policy (lines 5-6), which is the same as the traditional ϵ -greedy policy in Q-learning, where with probability β the greedy action is selected and with probability $1 - \beta$ a random action is selected, for exploration. We call it β -greedy to avoid confusion with our rare event probability ϵ .

Next, we obtain the importance weight w_t for this timeslot. The importance weight is the actual probability divided by the importance sampling - based probability (line 7). The temporal-difference (TD) error Δ_t will be updated (line 8), while involving error correction using the importance sampling weight w_t . With the TD-error, we update $\hat{Q}(s^t, a^t)$, the Q-value for state s^t and action a^t (line 9). The size of update is determined by the learning rate α^t . We then update either $T(s^t)$ or $U(s^t)$, depending on whether the next state s^{t+1} is a rare event state or not (lines 10-14). Finally, the importance sampling rare events probability $\hat{\epsilon}(s^t)$ is updated in line 15, according to $\frac{|T(s^t)|}{|T(s^t)|+|U(s^t)|}$, and bounded by δ and $1-\delta$. The process iterates for every timeslot, until we have achieved convergence. The converged policy will be applied online.

Algorithm 1 ImRE: Importance Sampling Q-Learning for Rare Events

```

1: Initialise:  $\hat{Q}(s, a)$  randomly,  $\hat{T}(s), \hat{U}(s) \leftarrow 0$ ,  $\hat{\epsilon}(s) \leftarrow \frac{1}{2}$ ,  $\alpha_T^t, \alpha_U^t$ .
2: Select the initial state  $s^0$  and action  $a^0$ .
3: for all timeslots  $t$  do
4:    $\hat{\epsilon}(s^t)$  determines if a rare event happens. Thereafter, sample according to  $h(\tilde{s}|s, a)$ . The new state  $s^{t+1}$  and a reward value  $r^{t+1} = r(s^t, a^t, s^{t+1})$  is observed.
5:    $a^{t+1} \leftarrow \beta - \text{greedy}(s^{t+1})$ .
6:    $a^* \leftarrow \text{argmax}_b \hat{Q}(s^{t+1}, b)$ .
7:    $w_t \leftarrow \begin{cases} \epsilon(s^t)/\hat{\epsilon}(s^t), & \text{if } s^{t+1} \in T. \\ (1 - \epsilon(s^t))/(1 - \hat{\epsilon}(s^t)), & \text{if } s^{t+1} \notin T. \end{cases}$ 
8:    $\Delta_t \leftarrow w_t(r^{t+1} + \gamma \hat{Q}(s^{t+1}, a^*) - \hat{Q}(s^t, a^t))$ 
9:    $\hat{Q}(s^t, a^t) \leftarrow \hat{Q}(s^t, a^t) + \alpha^t \Delta_t$ .
10:  if  $s^{t+1} \in T$  then
11:     $T(s^t) \leftarrow (1 - \alpha_T^t)T(s^t) + \alpha_T^t \epsilon(s^t)(r^{t+1} + \gamma \hat{Q}(s^{t+1}, a^*))$ 
12:  else
13:     $U(s^t) \leftarrow (1 - \alpha_U^t)U(s^t) + \alpha_U^t (1 - \epsilon(s^t))(r^{t+1} + \gamma \hat{Q}(s^{t+1}, a^*))$ 
14:  end if
15:   $\hat{\epsilon}(s^t) \leftarrow \min(\max(\delta, \frac{|T(s^t)|}{|T(s^t)|+|U(s^t)|}), 1 - \delta)$ 
16: end for

```

Our algorithm works for the scenario where $\exists s, s.t. |T(s)| \gg 0$. See Statement 2 in the definition of rare events in Definition 1. This condition means that the rare events have a sizeable contribution to the Q-value of at least one other state action pair (s, a) , and hence collectively have a sufficient impact on the reward/cost of the system. When this condition is not met, the cost of rare events to the users and network operator is not sufficiently high enough, resulting in less of a need to deal with rare events and use importance sampling to capture their impact on the cost.

6.3 Proofs of Boundedness and Convergence to Optimality

In this subsection, we prove the convergence of **ImRE**, our importance sampling based Q-learning algorithm (Algorithm 1).

Firstly, we show that the sequence of updates in Algorithm 1 is bounded, in the following theorem. We provide a summarized version of the proof here, with its full version

in our Technical Report [45]. The main idea of the proof is as follows: We rewrite Algorithm 1's update equation, through adding and subtracting terms. We rewrite the equation in the form of $\hat{Q}^{t+1}(s, a) = \hat{Q}^t(s, a) + \alpha^t [F_{s,a}(\hat{Q}^t) - \hat{Q}^t(s^t, a^t) + M_s(t)]$. Invoking Theorem 1 of [46] on stochastic approximation algorithms, we finally prove convergence by showing that the conditions for the sequence $F_{s,a}(\hat{Q})$ to be bounded are met.

Theorem 2. *For stepsizes following the conditions $\sum_t \alpha(t) = \infty$ and $\sum_t \alpha^2(t) \leq \infty$, and discount factor $\gamma \in (0, 1)$, the sequence of the \hat{Q} updates in Algorithm 1 is bounded, with probability 1.*

Proof. Algorithm 1's update equation is

$$\hat{Q}(s^t, a^t) \leftarrow \hat{Q}(s^t, a^t) + \alpha[w_t(r^{t+1} + \gamma \hat{Q}(s^{t+1}, a^*)) - \hat{Q}(s^t, a^t)], \quad (35)$$

where $a^* = \text{argmax}_b \hat{Q}(s^{t+1}, b)$.

We rewrite Algorithm 1's update equation through adding and subtracting the term $\sum_{s' \in S} \hat{p}(s'|s^t, a^t)(r^t(s^t, a^t, s') + \gamma \max_y \hat{Q}^t(s', y))$.

$\hat{Q}^{t+1}(s, a)$ can be further rewritten as

$$\hat{Q}^{t+1}(s, a) = \hat{Q}^t(s, a) + \alpha^t [F_{s,a}(\hat{Q}^t) - \hat{Q}^t(s^t, a^t) + M_s(t)],$$

for all (s, a) , where $F_{s,a} = [F_{s,1,a,1}, \dots, F_{s \times A,1}]^T$ is defined by

$$\begin{aligned} F_{s,a}(\hat{Q}^t(s, a)) \\ = \sum_{s' \in S} \hat{p}(s'|s, a)(r^t(s, a, s') + \gamma \max_y \hat{Q}^t(s', y)), \end{aligned}$$

and $\{M(t)\}$, $M(t) = [M_{1,1}(t), M_{1,2}(t), \dots, M_{|S \times A|}(t)]$ is a sequence of random vectors in $\mathbb{R}^{|S \times A|}$ satisfying

$$\mathbb{E}[M_m(t) | m < t] = 0$$

$$\|M(t)\| \leq K(1 + \|\hat{Q}^t\|)$$

for some constant $K > 0$. $\|M(t)\|$ is bounded because the probabilities $\epsilon(s^t)$ and $1 - \epsilon(s^t)$ are fixed, while $\hat{\epsilon}(s^t)$ and hence $1 - \hat{\epsilon}(s^t)$ are bounded in our algorithm (line 15). This results in the importance weight w^t (Eq. (33)) being bounded.

We show that the property $\|F(\hat{Q})\|_\infty \leq b\|\hat{Q}\|_\infty + d$ holds, where $\|\cdot\|_\infty$ is the supremum norm.

$$\begin{aligned} \|F(\hat{Q})\|_\infty \\ = \max_{i,a} \left| \sum_{s' \in S} \hat{p}(s'|i, a)(r(i, a, s') + \gamma \max_y \hat{Q}(s', y)) \right| \end{aligned} \quad (36)$$

$$\begin{aligned} &\leq \max_{i,a} \left| \sum_{s' \in S} \hat{p}(s'|i, a)r(i, a, s') \right| \\ &+ \left| \sum_{s' \in S} \hat{p}(s'|i, a)\gamma \max_y \hat{Q}(s', y) \right| \end{aligned} \quad (37)$$

$$\begin{aligned} &\leq \max_{i,a} \left| \sum_{s' \in S} \hat{p}(s'|i, a)r(i, a, s') \right| \\ &+ \gamma \max_{i,a} \left| \sum_{s' \in S} \hat{p}(s'|i, a) \max_{z,y} \hat{Q}(z, y) \right| \end{aligned} \quad (38)$$

$$\begin{aligned} &= \max_{i,a} \left| \sum_{s' \in S} \hat{p}(s'|i, a)r(i, a, s') \right| + \gamma \max_{i,a} \sum_{s' \in S} \hat{p}(s'|i, a) \|\hat{Q}\|_\infty \\ &= b\|\hat{Q}\|_\infty + d \end{aligned}$$

where $b = \gamma \max_{i,a} \sum_{s' \in S} \hat{p}(s'|i,a) = \gamma < 1$ and $d = \max_{i,a} |\sum_{s' \in S} \hat{p}(s'|i,a)r(i,a,s')| = \max_{i,a} |r(i,a,s')|$. The first inequality (from Eq. (36) to (37)) is true by the triangle inequality. Therefore, by Theorem 1 of [46] on stochastic approximation algorithms, the sequence of \hat{Q} updates in Algorithm 1 is bounded, with probability 1. \square

Next, to help us prove that our algorithm ImRE converges to optimality, we invoke the following theorem from [47]:

Corollary 3. *The random process $\{\Delta_t\}$ taking values in \mathbb{R}^n and defined as*

$$\Delta_{t+1}(x) = (1 - \alpha_t(x))\Delta_t(x) + \alpha_t F_t(x) \quad (39)$$

converges to zero with probability 1 when the following assumptions hold:

$$0 \leq \alpha_t \leq 1, \sum_t \alpha_t(x) = \infty \text{ and } \sum_t \alpha_t^2(x) < \infty.$$

$$||\mathbb{E}[F_t(x)]|| \leq \gamma ||\Delta_t||, \text{ where } \gamma < 1.$$

$$\text{var}[F_t(x)] \leq C(1 + ||\Delta_t||^2), \text{ for } C > 0.$$

In the following theorem, we show that our algorithm converges, and that it converges to the optimal policy. We provide a summarized version of the proof here, with its full version in our Technical Report [45]. The main idea of the proof is as follows. Firstly, we show that the optimal policy of the true system is a fixed point of the following equation with our simulator's transition probability $\hat{p}(s'|s,a)$ and the importance sampling correction weight $w_t(s)$: $Q^*(s,a) = \sum_{s' \in S} \hat{p}(s'|s,a)w_t(s)[r(s,a,s') + \gamma \max_b Q^*(s',b)]$. We define the operator $\mathbf{H}\hat{Q} = \sum_{s' \in S} \hat{p}(s'|s,a)w_t(s)[r(s,a,s') + \gamma \max_b \hat{Q}(s',b)]$, and show that $\mathbf{H}\hat{Q}$ is a contraction mapping. Next, we invoke the result of Corollary 3 on the convergence of random processes. We rewrite the update equation of Algorithm 1, such that it fits the form of Eq. (39) in Corollary 3, and show that the conditions of Corollary 3 hold, using the fact that $\mathbf{H}\hat{Q}$ is a contraction mapping.

Theorem 4. *If the MDP underlying the reinforcement learning environment is unichain for $\epsilon \in (\delta, 1-\delta)$,¹ for stepsizes following the conditions $0 \leq \alpha_t \leq 1$, $\sum_t \alpha_t(t) = \infty$ and $\sum_t \alpha_t^2(t) \leq \infty$, and discount factor $\gamma \in (0,1)$, Algorithm 1 converges to the optimal policy Q^* .*

Proof. Algorithm 1's update equation is

$$\begin{aligned} \hat{Q}^{t+1}(s^t, a^t) &\leftarrow \hat{Q}^t(s^t, a^t) + \alpha[w_t(r^{t+1} + \gamma \hat{Q}^t(s^{t+1}, a^*)) \\ &\quad - \hat{Q}^t(s^t, a^t)], \end{aligned} \quad (40)$$

where $a^* = \arg\max_b \hat{Q}(s^{t+1}, b)$.

By definition, the optimal policy Q^* of the true system with transition probability $p(s'|s,a)$ is a fixed point of the Bellman optimality equation:

$$Q^*(s,a) = \sum_{s' \in S} p(s'|s,a)[r(s,a,s') + \gamma \max_b Q^*(s',b)].$$

1. $(\delta, 1-\delta)$ is the range of values which $\hat{\epsilon}$ takes, as defined in Algorithm 1. If the MDP defined by transition probability $p(s'|s,a)$ is unichain for one value in $(\delta, 1-\delta)$, it is unichain for all values [20].

$\hat{p}(s'|s,a)$ is the transition probability in our simulator which incorporates importance sampling. $\hat{p}(s'|s,a) = \begin{cases} (1 - \hat{\epsilon}(s))h(\tilde{s}|s,a), & \text{if } s' \notin T \\ \hat{\epsilon}(s)h(\tilde{s}|s,a), & \text{if } s' \in T, \end{cases}$ as importance sampling of rare events takes place according to $\hat{\epsilon}(s)$. Without loss of generality, when we look at the case where s' is a rare state ($s' \in T$), we have

$$\begin{aligned} \hat{p}(s'|s,a)w_t(s) &= \hat{\epsilon}(s)h(\tilde{s}|s,a) \frac{\epsilon(s)}{\hat{\epsilon}(s)} \\ &= p(s'|s,a), \end{aligned}$$

the actual transition probability of the system. Therefore, since $p(s'|s,a) = \hat{p}(s'|s,a)w_t(s)$, the optimal policy Q^* is a fixed point of the following equation with our simulator's transition probability $\hat{p}(s'|s,a)$ and the importance sampling correction weight $w_t(s)$:

$$Q^*(s,a) = \sum_{s' \in S} \hat{p}(s'|s,a)w_t(s)[r(s,a,s') + \gamma \max_b Q^*(s',b)]. \quad (41)$$

We define the operator \mathbf{H} for a generic function \hat{Q}_i as

$$(\mathbf{H}\hat{Q})(s,a) = \sum_{s' \in S} \hat{p}(s'|s,a)w_t(s)[r(s,a,s') + \gamma \max_b \hat{Q}(s',b)]. \quad (42)$$

We have shown above that $\mathbf{H}Q^* = Q^*$. Now we show that \mathbf{H} is a contraction mapping. Note that both $\hat{p}(s'|s,a)$ and $w_t(s)$ are functions of \hat{Q} , because they are functions of $\hat{\epsilon}$, which is obtained as a function of \hat{Q} (algorithm lines 10-15). Nevertheless, we are able to prove contraction mapping because the product $\hat{p}(s'|s,a)(\hat{Q}) \times w_t(s(\hat{Q}))$ is the true transition probability $p(s'|s,a)$.

$$||\mathbf{H}\hat{Q}_1 - \mathbf{H}\hat{Q}_2||_\infty \quad (43)$$

$$\begin{aligned} &= \max_{s,a} | \sum_{s'} p(s'|s,a)[r(s,a,s') + \gamma \max_b \hat{Q}_1(s',b)] \\ &\quad - \sum_{s'} p(s'|s,a)[r(s,a,s') + \gamma \max_b \hat{Q}_2(s',b)] | \\ &\leq \max_{i,a} \gamma \sum_{s' \in S} p(s'|i,a) | \max_y \hat{Q}_1(s',y) - \max_y \hat{Q}_2(s',y) | \\ &\leq \max_{i,a} \gamma \sum_{s' \in S} p(s'|i,a) | \max_y |\hat{Q}_1(s',y) - \hat{Q}_2(s',y)| | \\ &\leq \max_{i,a} \gamma \sum_{s' \in S} p(s'|i,a) \max_{z,y} |\hat{Q}_1(z,y) - \hat{Q}_2(z,y)| \\ &= \max_{i,a} \gamma \sum_{s' \in S} p(s'|i,a) ||\hat{Q}_1 - \hat{Q}_2||_\infty \\ &= \gamma ||\hat{Q}_1 - \hat{Q}_2||_\infty, \end{aligned} \quad (44)$$

where $\gamma \in [0,1)$ according to the theorem conditions. The first inequality is true by the triangle inequality. The second inequality holds because $\max_x f(x) - \max_x g(x) \leq \max_x |f(x) - g(x)|$. Hence, we have shown that operator \mathbf{H} is a contraction mapping.

To prove convergence of our algorithm, we use the result from Corollary 3. Firstly, we subtract $Q^*(s^t, a^t)$ from both sides of Eq. (40), and letting $\Delta_t(s,a) = \hat{Q}^t(s,a) - Q^*(s,a)$, we have:

$$\begin{aligned} \Delta_{t+1}(s^t, a^t) &= (1 - \alpha^t)\Delta_t(s^t, a^t) + \alpha^t[w_t(r^{t+1} \\ &\quad + \gamma \max_b \hat{Q}^t(s^{t+1}, b)) - Q^*(s^t, a^t)], \end{aligned}$$

where $r^{t+1} = r(s^t, a^t, s^{t+1})$. Let $G_t(s, a) = w^t[r(s, a, X(s, a)) + \gamma \max_b \hat{Q}^t(X(s, a), b)] - Q^*(s, a)$, where $X(s, a)$ is a random sample obtained from the markov chain with state space S and transition probability $\hat{p}(s'|s, a)$ (the importance sampling modified transition probability). Taking the expectation, we have

$$\begin{aligned} \mathbb{E}[G_t(s, a)] &= \sum_{s' \in S} \hat{p}(s'|s, a) w^t(s, a, s') [r(s, a, s') + \gamma \max_b \hat{Q}^t(s', b)] \\ &\quad - Q^*(s, a) \\ &= \mathbf{H} \hat{Q}^t(s, a) - Q^*(s, a) \\ &= \mathbf{H} \hat{Q}^t(s, a) - \mathbf{H} Q^*(s, a). \end{aligned}$$

The last equality holds because Q^* is a fixed point of operator \mathbf{H} , as we have shown in Eqs. (41) and (42). Since we have shown that \mathbf{H} is a contraction mapping above, we have

$$\|\mathbb{E}[G_t(s, a)]\|_\infty \leq \gamma \|\hat{Q}^t(s, a) - Q^*\|_\infty = \gamma \|\Delta_t\|_\infty. \quad (45)$$

It remains to show that $\text{var}[G_t(s, a)] \leq C(1 + \|\Delta_t\|^2)$, for $C > 0$, where var refers to the variance.

$$\begin{aligned} \text{var}[G_t(s, a)] &= \mathbb{E} \left[\left(w^t[r(s, a, X(s, a)) + \gamma \max_b \hat{Q}^t(X(s, a), b)] \right. \right. \\ &\quad \left. \left. - \mathbf{H} \hat{Q}^t(s, a) \right)^2 \right] \\ &= \text{var} \left(w^t[r(s, a, X(s, a)) + \gamma \max_b \hat{Q}^t(X(s, a), b)] \right) \end{aligned}$$

Since w^t and r are bounded, we have

$$\text{var}[G_t(s, a)] \leq C(1 + \|\Delta_t\|_\infty^2)$$

for some constant $C > 0$. With this, we have shown the convergence of Algorithm ImRE. \square

Rare Event Adaptive Eligibility Traces Algorithm (ETAA, Algorithm 2): To speed up convergence for the tabular Q learning algorithm, we propose another variant of Algorithm 1 using eligibility traces. This algorithm (ETAA) is a combination of our proposed importance sampling based Q-learning Algorithm 1 and Watkin's $Q(\lambda)$ [48], which is an algorithm which combines Q-learning with eligibility traces. In this algorithm, $\hat{Q}(s, a)$ is updated for many combinations of (s, a) , at every time-slot, which helps to speed up convergence. Firstly, when we visit state s^t and take action a^t , we add one to the eligibility traces, as seen in line 5. Next, the eligibility traces will be decayed according to the factor λ :

$$e(s, a) \leftarrow \gamma \lambda e(s, a) w_t, \quad (46)$$

as seen in line 14, where γ is the reward discount factor and w_t is the importance weight. This means that the more recently we have visited (s, a) , the larger $e(s, t)$ will be, as less decaying has taken place. Next, the larger $e(s, t)$ is, the more $\hat{Q}(s, a)$ is updated by the TD-error Δ_t , as seen in line 7. If the action taken is not the greedy action, i.e., exploration has taken place, the eligibility traces will be set to 0, as seen in line 16. The rest of the algorithm follows Algorithm 1.

Corollary 5 states that ETAA remains bounded, for the case where $\lambda = 1$. Its proof is in our technical report [45].

Corollary 5. *The eligibility traces Q-Learning algorithm (ETAA), Algorithm 2 is bounded for the case $\lambda = 1$.*

Algorithm 2 ETAA: Eligibility Traces Rare Events-Adaptive Algorithm

```

1: Initialise: Same variables as Algorithm 1, along with
   eligibility traces  $e(s, a)$ .
2: Select the initial state  $s^0$  and action  $a^0$ .
3: for all timeslots  $t$  do
4:   The procedure follows that of Algorithm 1.
5:   When we visit  $s^t$  and take action  $a^t$ ,  $e(s^t, a^t) \leftarrow$ 
      $e(s^t, a^t) + 1$ .
6:    $a^{t+1} \leftarrow \beta - \text{greedy}(s^{t+1})$ .
7:    $a^* \leftarrow \text{argmax}_b \hat{Q}(s^{t+1}, b)$ .
8:   if  $\hat{Q}(s^{t+1}, a^*) = \hat{Q}(s^{t+1}, a^{t+1})$  then
9:      $a^* \leftarrow a^{t+1}$ 
10:  end if
11:  for all  $(s, a)$  do
12:     $\hat{Q}(s, a) \leftarrow \hat{Q}(s, a) + \alpha e(s, t) \Delta_t$ .
13:    if  $a^{t+1} = a^*$  then
14:       $e(s, a) \leftarrow \gamma \lambda e(s, a) w_t$ 
15:    else
16:       $e(s, a) \leftarrow 0$ .
17:    end if
18:  end for
19: end for

```

7 ALGORITHMS FOR LARGE STATE AND ACTION SPACES

To handle large state spaces, as might be found in real-world edge computing networks that span one or more cities and surrounding suburbs, we propose two variants of Algorithm 1 using deep Q-learning (Algorithm ImDQL) and actor critic (Algorithm ImACRE) respectively. The codes are available online at [49].

Rare Event Adaptive Deep Q-learning algorithm (ImDQL, Algorithm 3): We modify and combine the classic deep reinforcement learning algorithm in [50] with our importance sampling based rare events adaptive algorithm (Algorithm 1) by proposing an importance sampling based loss function. We parameterize the $\hat{Q}(s, a)$ value function using neural networks. The loss function is

$$L(\theta) = \mathbb{E}_{s, a, s'} [w_t(r^{t+1} + \gamma \max_a \hat{Q}(s, a, \theta^-) - Q(s, a, \theta))^2], \quad (47)$$

where θ^- are the weights of the target neural network, θ are the weights of the predicted neural network, which are updated every iteration, and w_t is the importance sampling weight. The loss function is optimized via gradient descent in line 13. Here, we are trying to minimize the difference between the target $w_t(r^{t+1} + \gamma \max_a \hat{Q}(s, a, \theta^-))$ and the prediction $Q(s, a, \theta)$. Because the target variable does not change in deep learning, here the target network is updated only every K iterations (line 16), while the prediction network is updated every iteration. Having the target fixed for awhile helps in having stable training. The key idea which differentiates our algorithm from traditional deep reinforcement learning algorithms is that our target $w_t(r^{t+1} + \gamma \max_a \hat{Q}(s, a, \theta^-))$ is "error corrected" by the importance sampling weight w_t , and the rare event distribution is updated via T, U and $\hat{\epsilon}$. The variables $T, U, \hat{\epsilon}$ and w_t are updated in the same manner as the tabular algorithm

Algorithm 3 ImDQL: Importance Sampling for Rare Events using Deep Q Learning

```

1: Initialise:  $\hat{Q}(s, a, \theta^-)$  and  $Q(s, a, \theta)$  randomly,
    $\hat{T}(s), \hat{U}(s) \leftarrow 0, \hat{\epsilon}(s) \leftarrow \frac{1}{2}$ .
2: Select the initial state  $s^0$  and action  $a^0$ .
3: for all timeslots  $t$  do
4:    $\hat{\epsilon}(s^t)$  determines if an anomaly happens. Thereafter,
     sample according to  $h(\tilde{s}|s, a)$ . The new state  $s^{t+1}$  and a
     reward value  $r^{t+1} = r(s^t, a^t, s^{t+1})$  is observed.
5:    $a^{t+1} \leftarrow \beta - \text{greedy}(s^{t+1})$ .
6:    $a^* \leftarrow \text{argmax}_b Q(s^{t+1}, b, \theta)$ .
7:   if  $Q(s^{t+1}, a^*, \theta) = Q(s^{t+1}, a^{t+1}, \theta)$  then
8:      $a^* \leftarrow a^{t+1}$ 
9:   end if
10:   $w_t \leftarrow \begin{cases} \epsilon(s^t)/\hat{\epsilon}(s^t), & \text{if } s^{t+1} \in T. \\ (1 - \epsilon(s^t))/(1 - \hat{\epsilon}(s^t)), & \text{if } s^{t+1} \notin T. \end{cases}$ 
11:  target  $y \leftarrow w_t(r^{t+1} + \gamma \hat{Q}(s^{t+1}, a^*, \theta^-))$ 
12:   $\theta_{t+1} \leftarrow \theta_t + \alpha \nabla_{\theta} \mathbb{E}[y - Q(s, a, \theta)]^2$ 
13:   $T(s^t) \leftarrow (1 - \alpha_T)T(s^t) + \alpha_T \epsilon(s^t)(r^{t+1} + \gamma Q(s^{t+1}, a^*, \theta_{t+1}))$ 
14:   $U(s^t) \leftarrow (1 - \alpha_U)U(s^t) + \alpha_U(1 - \epsilon(s^t))(r^{t+1} + \gamma Q(s^{t+1}, a^*, \theta_{t+1}))$ 
15:   $\hat{\epsilon}(s^t) \leftarrow \min(\max(\delta, \frac{|T(s^t)|}{|T(s^t)| + |U(s^t)|}), 1 - \delta)$ 
16:  Every  $K$  steps, reset  $\hat{Q} = Q$ .
17: end for

```

(Algorithm 1), through using the output of the prediction net $Q(s, a, \theta)$ where the input is state s^{t+1} . The actions are also selected in the same manner as Algorithm 1, through using the output of the prediction net $Q(s, a, \theta)$ where the input is state s^t .

Rare Event Adaptive Actor Critic Algorithm (ImACRE, Algorithm 4): Neural networks are used to approximate the “actor” and “critic” functions [51]. The critic function estimates the value (network c), based on which the actor function updates the policy (network θ). The advantage function $A(s^t, a^t)$ (line 8) measures how good taking action a^t is, compared to taking the average action, at state s^t . It is a function of the reward r^{t+1} , the values $V(s^t)$ and $V(s^{t+1})$ (obtained from the critic network c , line 7). It is corrected by the importance sampling correction weight $w^t(s^t, a^t, s^{t+1})$ (line 8), because we perform importance sampling of rare events. Each iteration, $A(s^t, a^t)$ will be stored in the buffer (line 9). The variables $T, U, \hat{\epsilon}$ and w_t are updated in the same manner as the tabular algorithm (Algorithm 1). At the end of an epoch (K timeslots), both the actor and critic networks are optimized, via gradient descent. The gradients for the actor and critic networks, respectively, are:

$$\nabla_{\theta} \sum_{i=1}^K \left[\frac{1}{K} \log \pi_{\theta}(a^i | s^i) A(s^i, a^i) \right]. \quad (48)$$

$$\nabla_c \sum_{i=1}^K \frac{1}{K} [A(s^i, a^i)]^2. \quad (49)$$

Both gradients are functions of the advantage value, stored in the buffer every iteration (line 9).

Algorithm 4 ImACRE: Importance Sampling based Advantage Actor Critic for Rare Events

```

1: Initialise: parameters  $\theta, c$  randomly,  $\hat{T}(s), \hat{U}(s) \leftarrow 0$ ,
    $\hat{\epsilon}(s) \leftarrow \frac{1}{2}$ , learning rates  $\alpha_{\theta}, \alpha_c, \alpha_T, \alpha_U$ .
2: Select the initial state  $s^0$  and action  $a^0$ .
3: for all timeslots  $t$  do
4:    $\hat{\epsilon}(s^t)$  determines if an anomaly happens. Thereafter,
     sample according to  $h(\tilde{s}|s, a)$ . The new state  $s^{t+1}$  and a
     reward value  $r^{t+1} = r(s^t, a^t, s^{t+1})$  is observed.
5:   Sample next action  $a^{t+1} \sim \pi_{\theta}(a|s^{t+1})$ 
6:    $w^t \leftarrow \begin{cases} \epsilon(s^t)/\hat{\epsilon}(s^t), & \text{if } s^{t+1} \in T. \\ (1 - \epsilon(s^t))/(1 - \hat{\epsilon}(s^t)), & \text{if } s^{t+1} \notin T. \end{cases}$ 
7:    $V(s^t) \leftarrow c(s^t)$ 
8:   Advantage function  $A(s^t, a^t) \leftarrow r^{t+1} + \gamma V(s^{t+1}) - w^t(s^t, a^t, s^{t+1})V(s^t)$ 
9:   Store  $A(s^t, a^t)$  in buffer.
10:   $T(s^t) \leftarrow (1 - \alpha_T)T(s^t) + \alpha_T \epsilon(s^t)(r^{t+1} + \gamma V(s^{t+1}))$ 
11:   $U(s^t) \leftarrow (1 - \alpha_U)U(s^t) + \alpha_U(1 - \epsilon(s^t))(r^{t+1} + \gamma V(s^{t+1}))$ 
12:   $\hat{\epsilon}(s^t) \leftarrow \min(\max(\delta, \frac{|T(s^t)|}{|T(s^t)| + |U(s^t)|}), 1 - \delta)$ 
13:  for every  $K$  steps do
14:    Update policy parameters using data in buffer:
     $\theta \leftarrow \theta - \alpha_{\theta} \nabla_{\theta} \sum_{i=1}^K \left[ \frac{1}{K} \log \pi_{\theta}(a^i | s^i) A(s^i, a^i) \right]$ 
15:    Update critic  $c \leftarrow c - \alpha_c \nabla_c \sum_{i=1}^K \frac{1}{K} [A(s^i, a^i)]^2$ 
16:    Empty buffer.
17:  end for
18: end for

```

Both algorithms differ from traditional Deep Q learning and Actor Critic algorithms, as importance sampling of server failures is integrated.

8 ADAPTING TO HETEROGENEOUS RISK TOLERANCES

Edge computing users, application vendors, and network providers have different tolerances towards server failures and the resulting higher latency which occur. Some applications are highly latency sensitive, and any server failure has a significant impact on safety and smooth functioning of the application, e.g., obstacle detection in autonomous vehicles, or immersive outdoor sport applications. Other users with less urgent jobs may see less of a need for a failure-aware backup placement resilient solution, due to the extra costs when storing and migrating backups. To deal with these heterogeneous risk tolerances, one potential solution is to alter the failure cost when training the algorithm. Nevertheless, the same rare event with the same objective cost to the system may inspire different risk tolerances and different willingness to incur a preparation cost amongst different users. Therefore, we propose a mechanism that can cater to edge computing users of heterogeneous risk tolerances. It takes the users’ risk tolerance towards server failures as an input, and derives a joint service placement and backup placement policy, based on the users’ risk tolerance. With RiTA (Risk Tolerance-Adaptive Algorithm), we also do not need to re-train a new policy $Q_{riskAware}$ for every possible level of risk, which scales better to a wider variety of users.

Algorithm 5 RiTA: Risk Tolerance-Adaptive Algorithm

```

1: Input: User risk tolerance level  $\zeta \in [0, 1]$ 
2:  $p_{riskAware} \leftarrow \text{softmax}(Q_{riskAware}(s, a))$ 
3:  $p_{riskTaking} \leftarrow \text{softmax}(Q_{riskTaking}(s, a))$ 
4: for all timeslots  $t$  do
5:   State transition occurs according to  $p(s'|s, a)$  and  $\epsilon(s)$ .
6:   if  $\text{rand}() < \zeta$  then
7:     Sample an action according to  $p_{riskTaking}$ .
8:   else
9:     Sample an action according to  $p_{riskAware}$ 
10:  end if
11: end for

```

We present this algorithm in Algorithm 8 (RiTA). Firstly, RiTA takes the user's risk tolerance level, ζ as input. The lower a user's risk tolerance, the more the user wants to avoid the cost arising from server failure. The higher a user's risk tolerance, the less the user is willing to prepare for failure, as it incurs an additional storage and migration cost. Next, this algorithm converts $Q_{riskAware}$ to a vector of probabilities $p_{riskAware}$, where $Q_{riskAware}$ is the converged policy trained from one of our importance-sampling failure-adaptive Q-learning simulator algorithms (Algorithms 1, 3, 4 or 2). The algorithm also converts $Q_{riskTaking}$ to a vector of probabilities $p_{riskTaking}$, where $Q_{riskTaking}$ is the converged policy of a Q-learning algorithm that does not take into account rare events in modelling of their environment, and does not consider the possibility of backups. This represents the risk taking component, for users who do not want to plan for rare events during service migration.

Algorithm 8 is an online algorithm to be used in real-time scenarios. For each timeslot, the state transition occurs according to $p(s'|s, a)$, and rare events according to the true rare events probability $\epsilon(s)$. At each timeslot, the policy which is used will be in accordance with the risk tolerance level $\zeta \in [0, 1]$. The lower the risk tolerance ζ , the higher the probability that the action selected will be sampled according to $p_{riskAware}$ (lines 6-10), which is obtained from our algorithm's converged policy. When $\zeta = 0$, the action selected will be according to our algorithm's converged policy. In the following theorem, we characterize the condition under which it would have been beneficial to prepare for rare events.

Theorem 6. After T time-slots, at risk level ζ , and under our algorithm, assuming our algorithm is able to prevent the cost of failures with probability $1 - f$, it benefited the user to prepare for rare events, if

$$F_c > \frac{N_c((\zeta - 1)f + \zeta)}{(\zeta - (1 - \zeta)f)} + \frac{T[(1 - \zeta)(N_c + B_c) - \zeta N_c] \sum_{i=0}^T \binom{T}{i} \epsilon^i (1 - \epsilon)^{T-i}}{(\zeta - (1 - \zeta)f) \sum_{i=0}^T \binom{T}{i} \epsilon^i (1 - \epsilon)^{T-i}},$$

where F_c, N_c, B_c respectively denote the average failure cost, normal state cost, and backup placement and migration cost.

Proof. The number of failures follow a binomial distribution with probability ϵ . We use this to model the expected cost of

preparation, and cost of not preparing for rare events. \square

9 SIMULATION EXPERIMENTS

In this section, we provide numerical evaluation for our algorithms ImRE, ImDQL, and ImACRE, validating, and going beyond the results in Section 6. In particular, we show that we have solved the main research challenges identified in Section 1. We show that our failure-adaptive importance sampling based algorithms *ImRE*, *ImDQL* and *ImACRE* converged to optimality. We also show that they were able to learn a policy which mitigates the high cost of server failures, unlike the baselines in which importance sampling or backups were not used, given a tradeoff of incurring a higher cost during normal states due to backup storage and migration. Moreover, we can adapt to varied risk tolerances without re-training. We perform our experiments with the help of real world traces [52].

We compare our algorithms with the following **baselines**, over 10 runs. Each of these baselines, besides the greedy baseline, may be trained with deep Q-learning or actor critic (to correspond to our algorithm). We will compare by applying the converged policy of each algorithm in an online scenario where the rare events occur at their true rate.

RL with No Importance-Sampling (NIS): This simulator is a traditional Q-learning algorithm where there is no importance sampling of rare events. Rare events are simulated at their true rate, and backups are a possible action. Comparison to this baseline indicates the role of importance sampling in helping the learned policy adapt to rare events.

RL without Backups as an Action (WBA): This simulator is a Q-learning algorithm in which there is no importance sampling of rare events and backups are not used as possible actions. Rare events are simulated at their true rate. Comparison to this baseline indicates the importance of backups in mitigating failure costs.

RL without Rare Events Sampled (RES): This simulator is a Q-learning algorithm under the "normal scenario", in which rare events are not modelled at all, during training. Likewise, backups are not considered as a possible action. Comparison to this baseline indicates the importance of including failures in the digital twin training environment.

Greedy Placement (GPM): Services and backups are placed at the top most likely locations of users, based on the current location of users, similar to reactive migration methods in the existing literature [53]. Comparison to this baseline indicates the importance of using learned policies instead of heuristics to optimize migration policies.

Single User Service Profile Migrations: In our experiments, we have 9 base stations (edge access points). The user is highly mobile across these coverage areas, and its mobility pattern follows a transition matrix. The ns-3 network simulator is used [52] to simulate dynamic channel network conditions, to obtain latency (delay) costs across different user-server location pairs. These latencies are in the range (2,10). As both the latency costs and migration costs are functions of the distance between user and access points, we set the migration cost $m_{ij} = d_{i,j}^{comm} + \epsilon$, where $\epsilon \in (-0.5, 0.5)$. We set the cost of failures to be -500,

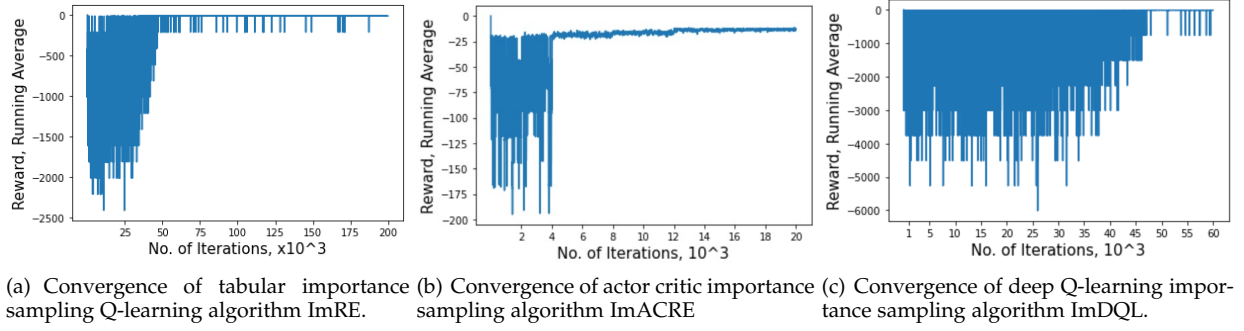


Fig. 3. Convergence of our proposed importance-sampling based rare events adaptive algorithms. Here, ImRE and ImACRE are applied to the a special case of the scenario (Section 3) where every user has their own service profile (the single user case), and ImDQL is applied to the scenario where users share service profiles (Section 3.2.2). All three variations of our algorithm converge.

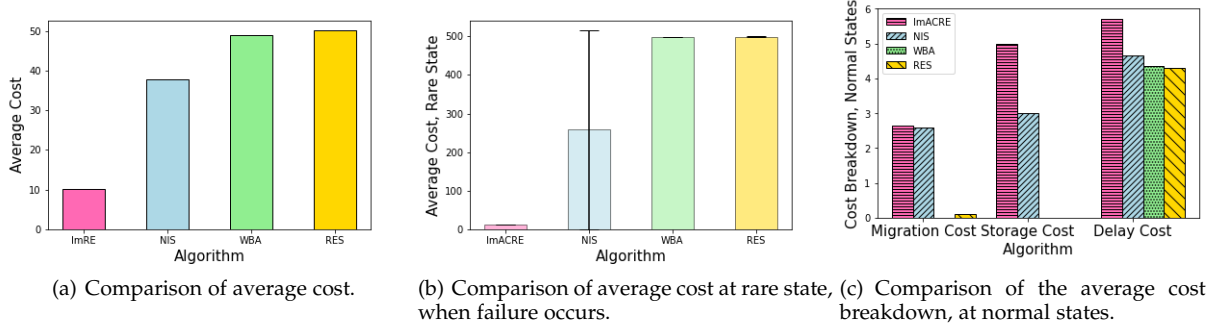


Fig. 4. **Single user service migration scenario:** Comparison of our actor critic algorithm importance sampling ImACRE, with actor critic versions of the baselines NIS, WBA and RES, in an online scenario. ImACRE leads to lower costs on average and in rare failure states, but higher storage and delay costs in normal states.

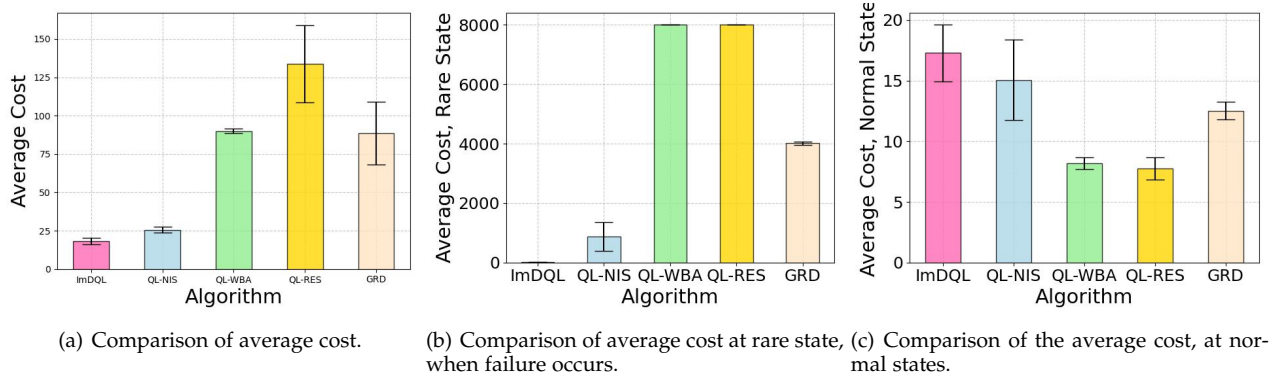


Fig. 5. **Multiple user service profile migrations:** Comparison of our deep Q-learning algorithm ImDQL, with baselines QL-NIS, QL-WBA and QL-RES, and greedy algorithm, in an online scenario. ImDQL yields much lower costs in rare states, yielding lower costs on average despite a slight increase in cost for normal states.

representing the high cost in terms of user experience or safety, and the true failure rate as 0.01. The learning rate used is 0.05 and both the actor and critic networks, for both our algorithms and the baselines, have a structure of [24, 48, 24] nodes per layer.

We apply our importance sampling based actor critic algorithm ImACRE and the corresponding actor critic baselines NIS, WBA, RES, for this scenario. In Fig. 3a, we show the convergence of ImACRE. In Fig. 4, we plot the overall average cost, average cost at rare states, and average cost at normal states, for our importance sampling based actor critic algorithm ImACRE and the corresponding actor critic baselines NIS, WBA, RES. All algorithms are run 10 times,

and the average is plot. Our algorithm achieves a lower average cost at rare states, because ImACRE sufficiently samples rare events to learn a policy which prepares for them. Our algorithm incurs a trade-off in terms of the higher normal state cost, especially incurred through the migration and storage of backups. It can be seen in Fig. 4b that Algorithm NIS avoids the elevated costs associated with rare events in certain runs. However, its performance exhibits a greater variability. WBA and RES incur the highest costs in rare events due to the absence of backup usage and the fact that rare events are entirely excluded from sampling during simulator training in the case of RES.

Multiple User Service Profile Migrations: In this sce-

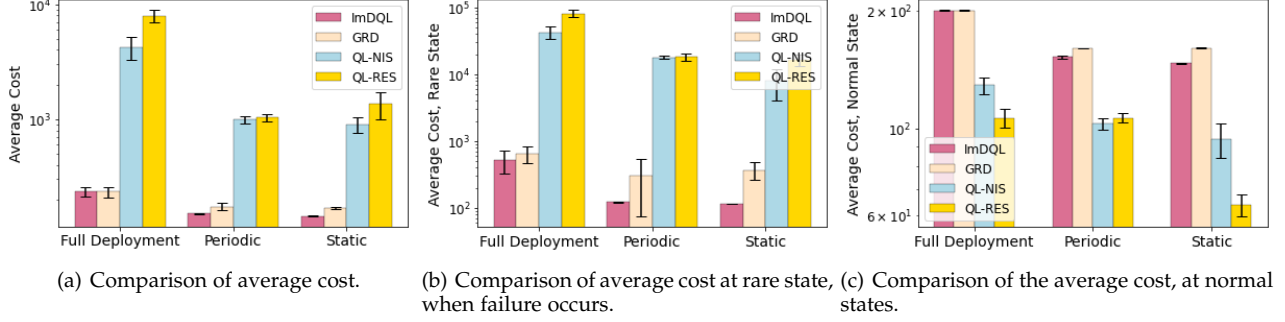


Fig. 6. **Shared service profile migrations:** Comparison of our deep Q-learning algorithm ImDQL, with baselines NIS, RES, and greedy algorithm, in three different settings. For all settings, our algorithm achieves a lower cost at rare states, and on average, than the baselines.

nario, we consider service profile migration for **multiple users**, where each user has their own service profile. We model 13 users mobile across 9 access points. Parameter settings are similar to the setup above. The natural failure rate is set to be 0.01. Users are mobile across the 9 APs, and their mobility patterns are sampled according to a transition probability matrix. We model different server failure types, corresponding to the differing amounts of maintenance resources available at each AP, which result in different amounts of time taken for the servers to come back online. For APs 1, 6, and 8, we let their service downtime be 2 time-slots per failure. For all other APs, we let their service downtime be 1 time-slot per failure. We apply algorithm ImDQL, our importance sampling based deep Q learning algorithm in this scenario.

In Fig. 5, we see that our ImDQL policy outperforms the baselines by achieving a lower average cost during rare states, with a trade-off of a higher average cost in normal (non-rare) states. Overall, our algorithm still achieves a lower cost, when averaged over all timeslots. QL-NIS and the greedy algorithm perform better than the other baselines, as backups are still a potential action for the algorithm in QL-NIS, and the greedy algorithm places one backup at the second most likely location every time-slot. Nevertheless these algorithms do not avoid the rare event cost as much as our algorithm does.

Shared service profiles: In this scenario (Fig. 6), we consider multiple users sharing the same service profile (SP). We model 100 users, with 70 users using SP Type 1, and 30 using SP Type 2. These users are spread over a 2-city map, which 2APs in one city and 3 in another. It has a failure cost of 1000 and failure rate of $1e-2$. If a user's required access point is in another city, the delay cost between cities will be nearly as large as the failure cost, which is much larger than the delay cost when accessing a service profile within the same city. We apply ImDQL to this scenario and compare its performance with NIS, RES and the greedy baseline. The greedy baseline deploys SPs to the N most probable places w.r.t distribution of user transitions, where we search through all N and plot the results with the lowest costs.

We look at 3 settings: a) *Full Deployment*, where users are spread across zones evenly. The greedy baseline's optimal solution is to fully deploy all SPs. b) *Periodic*, where users move across areas periodically, and c) *Static*, a corner case where users stay in their current zone. As seen in Fig. 6, in all settings, ImDQL achieves a lower cost in rare event

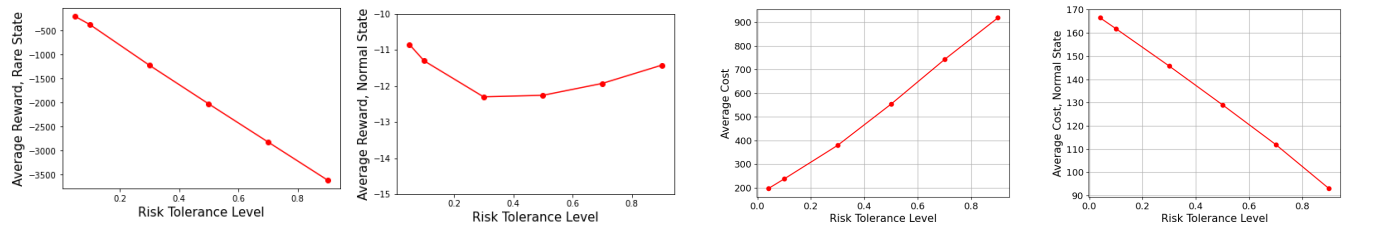
states, followed by GRD (greedy), as compared to QL-NIS and QL-RES, which place little or no backups. While there is a trade-off with a higher cost in normal states, on average over all states, ImDQL and GRD still achieve a lower cost (Fig. 6 a) than the other baselines. ImDQL outperforms GRD in the periodic and static settings, as the greedy baseline cannot adapt to the presence of rare failures that may occur in each city.

Catering to varying risk tolerances: We apply our algorithm RiTA (Algorithm 8), which caters to users having different risk tolerances. Given the risk tolerance level of a user ζ , with probability $1 - \zeta$, RiTA will select an action according to the converged policy of our algorithm ImRE (risk adverse component), and with probability ζ RiTA will select an action according to the converged policy of the baseline QL-RES (risk taking component). We apply RiTA to the single user (3 APs) service migration setting, which is a special case of the individual SP scenario, and to the multiple user shared SP scenario (5 APs across 2 cities).

In Fig. 7 we present how the risk tolerance level ζ impacts the reward levels. As seen in Figs. 7 a) and b), for the single user individual SP scenario, the higher the risk tolerance, the higher the cost experienced at rare states (as it is less likely backups were placed). For normal states, as the risk tolerance level ζ decreases from $\zeta = 1$, the cost first increases due to the increase in storage of backups (resulting from being increasingly risk adverse). After $\zeta = 0.3$, the cost decreases. This is because as ζ decreases, the weightage given to the risk adverse component (our algorithm ImRE) increases. While ImRE incurs a higher storage cost than RES, it manages to learn a policy in which frequent migrations do not occur, hence decreasing the normal state cost. For the shared service profile scenario, as the risk tolerance ζ increases, the cost at normal state decreases due to the placement of less services, while the average cost (over all states) increases. This is because multiple users share service profiles like game environments, multiplying the cost when failures occur.

10 CONCLUSION

In edge computing, server failures may spontaneously occur, which complicates resource allocation and service migration. While failures are considered as rare events, they have an impact on the smooth and safe functioning of edge computing's latency sensitive applications. As these failures



(a) Individual SP scenario: Average reward across rare states. (b) Individual SP scenario: Average reward across normal states. (c) Shared SP scenario: Average Cost across all states. (d) Shared SP scenario: Average Cost, normal states.

Fig. 7. **Heterogeneous Risk Tolerances:** Evaluating how the risk tolerance levels impact the cost, when Algorithm RiTA is applied. A higher risk tolerance leads to higher cost and lower reward in rare states, but may decrease the cost in normal states.

occur at a low probability, it is difficult to jointly plan or learn an optimal service migration solution for both the typical and rare event scenarios. Therefore, we introduce a rare events adaptive resilience framework named FIRE, using the placement of backups and importance sampling based reinforcement learning, which alters the sampling rate of rare events in order to learn an optimal risk-averse policy. We prove the boundedness and convergence to optimality of our proposed tabular Q-learning algorithm ImRE. To handle large and combinatorial state and action spaces common in real-world networks, we propose deep Q-learning (ImDQL) and actor critic (ImACRE) versions of our algorithm. Furthermore, we propose a decision making algorithm (RiTA) that caters to heterogeneous risk tolerances across users. Finally, we use trace driven experiments to show that our algorithms converge to optimality, and are resilient towards server failures, unlike several baselines, subject to a trade-off in terms of a potential higher normal state cost. Our framework can also be modified for other resource allocation problems pertaining rare events with large consequences in communication and networking.

REFERENCES

- [1] Y. Mao, C. You, J. Zhang, K. Huang, and K. B. Letaief, "A survey on mobile edge computing: The communication perspective," *IEEE Communications Surveys & Tutorials*, vol. 19, no. 4, pp. 2322–2358, 2017.
- [2] P. Mach and Z. Becvar, "Mobile edge computing: A survey on architecture and computation offloading," *IEEE Communications Surveys Tutorials*, vol. 19, no. 3, pp. 1628–1656, 2017.
- [3] Y. Mao, J. Zhang, and K. B. Letaief, "Dynamic computation offloading for mobile-edge computing with energy harvesting devices," *IEEE Journal on Selected Areas in Communications*, vol. 34, no. 12, pp. 3590–3605, 2016.
- [4] X. Chen, L. Jiao, W. Li, and X. Fu, "Efficient multi-user computation offloading for mobile-edge cloud computing," *IEEE/ACM Transactions on Networking*, vol. 24, no. 5, pp. 2795–2808, 2015.
- [5] T. Q. Dinh, J. Tang, Q. D. La, and T. Q. Quek, "Offloading in mobile edge computing: Task allocation and computational frequency scaling," *IEEE Transactions on Communications*, vol. 65, no. 8, pp. 3571–3584, 2017.
- [6] M. Siew, S. Sharma, K. Guo, D. Cai, W. Wen, C. Joe-Wong, and T. Q. Quek, "Towards effective resource procurement in mec: a resource re-selling framework," *IEEE Transactions on Services Computing*, 2023.
- [7] S. Wang, R. Ugaonkar, M. Zafer, T. He, K. Chan, and K. K. Leung, "Dynamic service migration in mobile edge computing based on markov decision process," *IEEE/ACM Transactions on Networking*, vol. 27, no. 3, pp. 1272–1288, 2019.
- [8] T. Ouyang, Z. Zhou, and X. Chen, "Follow me at the edge: Mobility-aware dynamic service placement for mobile edge computing," *IEEE Journal on Selected Areas in Communications*, vol. 36, no. 10, pp. 2333–2345, 2018.
- [9] S. Wang, J. Xu, N. Zhang, and Y. Liu, "A survey on service migration in mobile edge computing," *IEEE Access*, vol. 6, pp. 23 511–23 528, 2018.
- [10] K. Guo, R. Gao, W. Xia, and T. Q. Quek, "Online learning based computation offloading in mec systems with communication and computation dynamics," *IEEE Transactions on Communications*, vol. 69, no. 2, pp. 1147–1162, 2020.
- [11] S. Wang, Y. Guo, N. Zhang, P. Yang, A. Zhou, and X. Shen, "Delay-aware microservice coordination in mobile edge computing: A reinforcement learning approach," *IEEE Transactions on Mobile Computing*, vol. 20, no. 3, pp. 939–951, 2019.
- [12] B. Gao, Z. Zhou, F. Liu, F. Xu, and B. Li, "An online framework for joint network selection and service placement in mobile edge computing," *IEEE Transactions on Mobile Computing*, pp. 1–1, 2021.
- [13] T. Ouyang, R. Li, X. Chen, Z. Zhou, and X. Tang, "Adaptive user-managed service placement for mobile edge computing: An online learning approach," in *IEEE INFOCOM 2019-IEEE conference on computer communications*. IEEE, 2019, pp. 1468–1476.
- [14] M. Siew, K. Guo, D. Cai, L. Li, and T. Q. Quek, "Let's share vms: Optimal placement and pricing across base stations in mec systems," in *IEEE INFOCOM 2021-IEEE Conference on Computer Communications*. IEEE, 2021, pp. 1–10.
- [15] T. Kim, S. D. Sathyanarayana, S. Chen, Y. Im, X. Zhang, S. Ha, and C. Joe-Wong, "Modems: Optimizing edge computing migrations for user mobility," in *IEEE INFOCOM 2022-IEEE Conference on Computer Communications*. IEEE, 2022, pp. 1159–1168.
- [16] D. Zeng, L. Gu, S. Pan, J. Cai, and S. Guo, "Resource management at the network edge: A deep reinforcement learning approach," *IEEE Network*, vol. 33, no. 3, pp. 26–33, 2019.
- [17] Z. Gao, Q. Jiao, K. Xiao, Q. Wang, Z. Mo, and Y. Yang, "Deep reinforcement learning based service migration strategy for edge computing," in *2019 IEEE International Conference on Service-Oriented System Engineering (SOSE)*, 2019, pp. 116–1165.
- [18] L. Ponemon, "Cost of data center outages," *Data Center Performance Benchmark Serie*, 2016.
- [19] A. Aral and I. Brandić, "Learning spatiotemporal failure dependencies for resilient edge computing services," *IEEE Transactions on Parallel and Distributed Systems*, vol. 32, no. 7, pp. 1578–1590, 2020.
- [20] J. Frank, S. Mannor, and D. Precup, "Reinforcement learning in the presence of rare events," in *Proceedings of the 25th international conference on Machine learning*, 2008, pp. 336–343.
- [21] H. Hong, Q. Wu, F. Dong, W. Song, R. Sun, T. Han, C. Zhou, and H. Yang, "Netgraph: An intelligent operated digital twin platform for data center networks," in *Proceedings of the ACM SIGCOMM 2021 Workshop on Network-Application Integration*, 2021, pp. 26–32.
- [22] Y. Zhang, L. Jiao, J. Yan, and X. Lin, "Dynamic service placement for virtual reality group gaming on mobile edge cloudlets," *IEEE Journal on Selected Areas in Communications*, vol. 37, no. 8, pp. 1881–1897, 2019.
- [23] A. Aral and T. Ovatman, "A decentralized replica placement algorithm for edge computing," *IEEE Transactions on Network and Service Management*, vol. 15, no. 2, pp. 516–529, 2018.
- [24] T. Taleb and A. Ksentini, "An analytical model for follow me cloud," in *2013 IEEE Global Communications Conference (GLOBECOM)*, 2013, pp. 1291–1296.
- [25] A. Ksentini, T. Taleb, and M. Chen, "A markov decision process-based service migration procedure for follow me cloud," in *2014 IEEE ICC*, 2014, pp. 1350–1354.

- [26] S. N. Shirazi, A. Gouglidis, A. Farshad, and D. Hutchison, "The extended cloud: Review and analysis of mobile edge computing and fog from a security and resilience perspective," *IEEE Journal on Selected Areas in Communications*, vol. 35, no. 11, pp. 2586–2595, 2017.
- [27] C.-F. Liu, M. Bennis, M. Debbah, and H. V. Poor, "Dynamic task offloading and resource allocation for ultra-reliable low-latency edge computing," *IEEE Transactions on Communications*, vol. 67, no. 6, pp. 4132–4150, 2019.
- [28] H. Huang and S. Guo, "Proactive failure recovery for nfv in distributed edge computing," *IEEE Communications Magazine*, vol. 57, no. 5, pp. 131–137, 2019.
- [29] G. Yao, X. Li, Q. Ren, and R. Ruiz, "Failure-aware elastic cloud workflow scheduling," *IEEE Transactions on Services Computing*, pp. 1–14, 2022.
- [30] Y. Liang, Z. Hu, and L. Yang, "A two-stage replica management mechanism for latency-aware applications in multi-access edge computing," in *2021 IEEE Intl Conf on Parallel & Distributed Processing with Applications, Big Data & Cloud Computing, Sustainable Computing & Communications, Social Computing & Networking (ISPA/BDCloud/SocialCom/SustainCom)*. IEEE, 2021, pp. 453–459.
- [31] R. Zhang, F. R. Yu, J. Liu, T. Huang, and Y. Liu, "Deep reinforcement learning (drl)-based device-to-device (d2d) caching with blockchain and mobile edge computing," *IEEE Transactions on Wireless Communications*, vol. 19, no. 10, pp. 6469–6485, 2020.
- [32] W. Du, Q. He, Y. Ji, C. Cai, and X. Zhao, "Optimal user migration upon server failures in edge computing environment," in *2021 IEEE International Conference on Web Services (ICWS)*. IEEE, 2021, pp. 272–281.
- [33] M. Siew, S. Sharma, and C. Joe-Wong, "Acre: Actor critic reinforcement learning for failure-aware edge computing migrations," in *2023 57th Annual Conference on Information Sciences and Systems (CISS)*. IEEE, 2023, pp. 1–6.
- [34] P. A. Apostolopoulos, E. E. Tsiropoulou, and S. Papavassiliou, "Risk-aware data offloading in multi-server multi-access edge computing environment," *IEEE/ACM Transactions on Networking*, vol. 28, no. 3, pp. 1405–1418, 2020.
- [35] M. S. Munir, S. F. Abedin, N. H. Tran, Z. Han, E.-N. Huh, and C. S. Hong, "Risk-aware energy scheduling for edge computing with microgrid: A multi-agent deep reinforcement learning approach," *IEEE Transactions on Network and Service Management*, vol. 18, no. 3, pp. 3476–3497, 2021.
- [36] H. Badri, T. Bahreini, D. Grosu, and K. Yang, "Risk-aware application placement in mobile edge computing systems: A learning-based optimization approach," in *2020 IEEE International Conference on Edge Computing (EDGE)*, 2020, pp. 83–90.
- [37] X. Chen, H. Zhang, C. Wu, S. Mao, Y. Ji, and M. Bennis, "Optimized computation offloading performance in virtual edge computing systems via deep reinforcement learning," *IEEE Internet of Things Journal*, vol. 6, no. 3, pp. 4005–4018, 2018.
- [38] J. Zhang, X. Hu, Z. Ning, E. C.-H. Ngai, L. Zhou, J. Wei, J. Cheng, and B. Hu, "Energy-latency tradeoff for energy-aware offloading in mobile edge computing networks," *IEEE Internet of Things Journal*, vol. 5, no. 4, pp. 2633–2645, 2017.
- [39] D. Precup, "Eligibility traces for off-policy policy evaluation," *Computer Science Department Faculty Publication Series*, p. 80, 2000.
- [40] R. S. Sutton and A. G. Barto, *Reinforcement learning: An introduction*. MIT press, 2018.
- [41] U. Madhushani, B. Dey, N. E. Leonard, and A. Chakraborty, "Hamiltonian q-learning: Leveraging importance-sampling for data efficient rl," *arXiv preprint arXiv:2011.05927*, 2020.
- [42] L. Ma, S. Yi, and Q. Li, "Efficient service handoff across edge servers via docker container migration," in *Proceedings of the Second ACM/IEEE Symposium on Edge Computing*, 2017, pp. 1–13.
- [43] J. Wu, E. W. Wong, Y.-C. Chan, and M. Zukerman, "Energy efficiency-qos tradeoff in cellular networks with base-station sleeping," in *GLOBECOM 2017-2017 IEEE Global Communications Conference*. IEEE, 2017, pp. 1–7.
- [44] J. A. Bucklew and J. Bucklew, *Introduction to rare event simulation*. Springer, 2004, vol. 5.
- [45] "This paper's technical report." [Online]. Available: <http://tinyurl.com/RareEventsEC>
- [46] J. N. Tsitsiklis, "Asynchronous stochastic approximation and q-learning," *Machine learning*, vol. 16, no. 3, pp. 185–202, 1994.
- [47] T. Jaakkola, M. Jordan, and S. Singh, "Convergence of stochastic iterative dynamic programming algorithms," *Advances in neural information processing systems*, vol. 6, 1993.
- [48] C. J. C. H. Watkins, "Learning from delayed rewards," 1989.
- [49] "Code for algorithm imdql." [Online]. Available: <https://github.com/ShikhSh/MultiUser-FIRE>
- [50] V. Mnih, K. Kavukcuoglu, D. Silver, A. A. Rusu, J. Veness, M. G. Bellemare, A. Graves, M. Riedmiller, A. K. Fidjeland, G. Ostrovski et al., "Human-level control through deep reinforcement learning," *nature*, vol. 518, no. 7540, pp. 529–533, 2015.
- [51] V. Mnih, A. P. Badia, M. Mirza, A. Graves, T. Lillicrap, T. Harley, D. Silver, and K. Kavukcuoglu, "Asynchronous methods for deep reinforcement learning," in *International conference on machine learning*. PMLR, 2016, pp. 1928–1937.
- [52] "ns3 network simulator." [Online]. Available: <https://www.nsnam.org/>
- [53] Z. Rejiba, X. Masip-Bruin, and E. Marín-Tordera, "A survey on mobility-induced service migration in the fog, edge, and related computing paradigms," *ACM Computing Surveys (CSUR)*, vol. 52, no. 5, pp. 1–33, 2019.

Marie Siew is a Faculty Early Career Award (FECA) Fellow at the Singapore University of Technology and Design.

Shikhar Sharma was a Masters Student in ECE, Carnegie Mellon University.

Zekai Li is a Masters Student in ECE, Carnegie Mellon University.

Kun Guo is a Professor at East China Normal University, Shanghai, China.

Chao Xu is a Professor in Northwest A&F University, China.

Tania Lorida Botran is a Research Scientist at Roblox.

Tony Q.S. Quek is the Cheng Tsang Man Chair Professor with Singapore University of Technology and Design (SUTD) and ST Engineering Distinguished Professor.

Carlee Joe-Wong is the Robert E. Doherty Associate Professor of Electrical and Computer Engineering at Carnegie Mellon University.